



**HAL**  
open science

# The methylome of *Biomphalaria glabrata* and other mollusks: enduring modification of epigenetic landscape and phenotypic traits by a new DNA methylation inhibitor

Nelia Luviano, Marie Lopez, Fleur Gawehns, Cristian Chaparro, Paola B Arimondo, Slavica Ivanovic, Patrice David, Koen Verhoeven, Céline Cosseau, Christoph Grunau

## ► To cite this version:

Nelia Luviano, Marie Lopez, Fleur Gawehns, Cristian Chaparro, Paola B Arimondo, et al.. The methylome of *Biomphalaria glabrata* and other mollusks: enduring modification of epigenetic landscape and phenotypic traits by a new DNA methylation inhibitor. 2021. pasteur-03427775v1

**HAL Id: pasteur-03427775**

**<https://hal.science/pasteur-03427775v1>**

Preprint submitted on 27 May 2021 (v1), last revised 14 Nov 2021 (v2)

**HAL** is a multi-disciplinary open access archive for the deposit and dissemination of scientific research documents, whether they are published or not. The documents may come from teaching and research institutions in France or abroad, or from public or private research centers.

L'archive ouverte pluridisciplinaire **HAL**, est destinée au dépôt et à la diffusion de documents scientifiques de niveau recherche, publiés ou non, émanant des établissements d'enseignement et de recherche français ou étrangers, des laboratoires publics ou privés.

1 **The methylome of *Biomphalaria glabrata* and other mollusks:**  
2 **enduring modification of epigenetic landscape and phenotypic**  
3 **traits by a new DNA methylation inhibitor**

4 Nelia Luviano <sup>1</sup>, Marie Lopez <sup>2,3</sup>, Fleur Gawehns <sup>4</sup>, Cristian Chaparro <sup>1</sup>, Paola B. Arimondo <sup>3,5</sup>, Slavica  
5 Ivanovic <sup>6</sup>, Patrice David <sup>7</sup>, Koen Verhoeven <sup>6</sup>, Céline Cosseau <sup>1</sup>, Christoph Grunau <sup>1</sup>

6  
7 <sup>1</sup> Interactions Hôtes Pathogènes Environnements (IHPE), Univ. Montpellier, CNRS, Ifremer, Univ.  
8 Perpignan Via Domitia, Perpignan France

9  
10 <sup>2</sup> Institut des Biomolécules Max Mousseron (IBMM), CNRS, Univ Montpellier, ENSCM UMR 5247, 240  
11 avenue du Prof. E. Jeanbrau, 34296 Montpellier cedex 5, France

12 <sup>3</sup> Epigenetic Targeting of Cancer (ETaC), CNRS FRE3600, Centre de Recherche et Développement  
13 Pierre Fabre, Toulouse, France

14 <sup>4</sup> Bioinformatics Unit, Netherlands Institute of Ecology (NIOO-KNAW), Wageningen, The  
15 Netherlands.

16 <sup>5</sup> Epigenetic Chemical Biology (EpiChBio), Department Structural Biology and Chemistry, UMR 3523  
17 CNRS, Institute Pasteur, 75015 Paris, France

18 <sup>6</sup> Department of Terrestrial Ecology, Netherlands Institute of Ecology (NIOO-KNAW), Wageningen,  
19 The Netherlands.

20 <sup>7</sup> Centre d'Ecologie Fonctionnelle et Evolutive (CEFE), Univ. Montpellier, CNRS - - Université Paul  
21 Valéry Montpellier - EPHE, 1919 Route de Mende, 34293 Montpellier Cedex 5, France

22 \* To whom correspondence should be addressed. Tel: +33(0)4-68-66-21-80; Email:  
23 christoph.grunau@univ-perp.fr

24 **Abstract**

25 5-methylcytosine (5mC) is an important epigenetic mark in eukaryotes. Little information about its  
26 role exists for invertebrates. How 5mC contributes to phenotypic variation in invertebrates can be  
27 investigated by experimental alteration of methylation patterns. Here, we apply new non-nucleoside  
28 DNA methyltransferase inhibitors (DNMTi) to introduce global changes into the methylome of  
29 mollusk species. Flavanone inhibitor Flv1 was highly efficient in reducing 5mC in the freshwater snails  
30 *Biomphalaria glabrata* and *Physa acuta*, and to a lesser degree, probably due to lower stability in sea  
31 water, in the oyster *Crassostrea gigas*. Flv1 has no toxic effects and significantly decreased the 5mC  
32 level in the treated *B. glabrata* generation and in its untreated offspring. Drug treatment triggers  
33 significant variation in the morphometric traits in both generations. An epigenotyping by sequencing  
34 method corroborates hypomethylation effect of Flv1 in both *B. glabrata* generations and identifies  
35 one Differential Methylated Region (DMR) out of 8, found both in Flv1-exposed snails and its

36 progeny, demonstrating a multigenerational effect of an induced epimutation. By targeted bisulfite  
37 sequencing, we confirmed hypomethylation in a *locus* associated with reduced gene expression.

38 **Keywords:** DNMT inhibitors, 5-methylcytosine, mollusks, Invertebrates, epigenetic inheritance,  
39 epimutation.

#### 40 **Background**

41 DNA methylation is an epigenetic mark that can be associated with changes in gene function without  
42 changes in the underlying DNA sequence (Ganesan, Arimondo, Rots, Jeronimo, & Berdasco, 2019).

43 Modifications in DNA methylation can be induced by the environment and some changes can be  
44 mitotically and/or meiotically heritable and/or are reversible (Dupont, Armant, and Brenner 2009,

45 Nicoglou and Merlin 2017). Some of these modifications can influence gene function by providing  
46 differential access to the underlying genetic information in cells, and thus may alter their

47 phenotypes. Epigenetic marks such as DNA methylation may provide an additional dimension to  
48 inheritance, linked to but different from genetic inheritance. Epimutations can be provoked directly

49 by environmental stresses and contribute to rapid evolutionary changes but unlike genetic variation,  
50 epimutations have higher rates and are reversible (Bossdorf, Richards, and Pigliucci 2008, Cosseau et

51 al. 2017). Biochemically, DNA methylation is the modification of a DNA base, and is present in a  
52 diverse range of eukaryotic organisms, ranging from *fungi* to mammals (Chen 2011). One type of

53 DNA methylation is cytosine methylation that is catalyzed by the DNA methyltransferases (DNMTs),  
54 enzymes that transfer the methyl group (-CH<sub>3</sub>) from the co-substrate S-adenosyl-L-methionine (SAM)

55 to the carbon-5 of the cytidine, to form 5-methylcytidine (5mC) (Moore, Le, and Fan 2013). In  
56 vertebrates, DNA methylation occurs on cytosines in a CpG context (cytidine followed by a

57 guanosine) (Li and Zhang 2014) whereas, DNA methylation can also occur in CHH and CHG (H=A, T, C)  
58 context (Meng et al. 2015) in plants. Less is known about the methylation in invertebrates, though

59 many species present DNA methylation in a CpG context (Glastad et al. 2011).

60 DNA methylation is assumed to be evolutionary ancient, but its function and pattern is very  
61 diversified. This is consistent with the notion of a dynamically evolving mechanism that can adapt to  
62 perform various functions (Zilberman 2008), but having a common origin and being always part of an  
63 inheritance system (Aliaga et al. 2019). Major differences in DNA methylation are observed among  
64 phyla (Keller, Han, and Yi 2016). In the animal kingdom, vertebrates have one of the highest levels of  
65 DNA methylation that is uniformly spread all over the genome and found in all sorts of genomic  
66 contexts such as gene bodies, gene promoters, intergenic regions and repetitive DNA such as  
67 transposons (Suzuki and Bird 2008) (“global methylation”). Only promoter sequences are generally  
68 unmethylated and methylation here has been demonstrated to modulate gene expression in cis.  
69 Methylation also affects DNA repair stability, splicing, imprinting, development, germ cell  
70 pluripotency and cell fate (Schübeler 2015). In contrast, in many invertebrates, a common type of  
71 DNA methylation is the “mosaic” pattern consisting in large domains of methylated DNA separated  
72 by large domains of unmethylated DNA (Hendrich and Tweedie 2003). Another pattern observed is a  
73 very low level (Gowher, Leismann, and Jeltsch 2000) or a total absence of DNA methylation (Capuano  
74 et al. 2014, Aliaga et al. 2019). When methylation is of mosaic type, 5mC is often found in genes (in  
75 exons and sometimes to a lesser degree in introns), a type of methylation also called Gene Body  
76 Methylation (GBM). GBM is considered as the ancestral form of DNA methylation (Feng et al. 2010).  
77 Higher GBM is believed to be associated with active transcription in vertebrates and invertebrates,  
78 while promoter methylation in vertebrates is associated with repression of gene expression (Sarda et  
79 al. 2012).

80

81 An important aspect of epigenetic marks is their inheritance. There is evidence in model species,  
82 mainly plants (Johannes et al. 2009), that heritable variation in ecologically important traits can be  
83 generated through changes in DNA methylation and that these changes may be inherited to future  
84 generations. Nevertheless, in contrast to plants and vertebrates, there is little evidence of

85 transgenerational stability of DNA methylation in invertebrates. Consequently, more evidence is  
86 needed about whether environmental-based DNA methylation changes can be inherited across  
87 generations in invertebrates and in here we focused on this question in mollusks. DNA methylation  
88 has been relatively little investigated in mollusks as discussed in (Fallet, Luquet, David, & Cosseau,  
89 2020), where information is essentially based on data from two species: the pacific oyster  
90 *Crassostrea gigas* and the freshwater snail *Biomphalaria glabrata*. In the abovementioned work,  
91 authors distinguish the terms multigenerational and transgenerational. Multigenerational effect  
92 results from a direct exposure of the germline, gametes or embryos to the environmental stress,  
93 while a transgenerational effect involves a germ line transmission between generations without  
94 direct exposure to the environmental stress (Fallet et al. 2020). In this work, we investigated these  
95 two mollusks species and added the previously unstudied *Physa acuta*, i.e. three molluscan models of  
96 medical, economic and ecological importance.

97

98 The snail *B. glabrata* is the intermediate host of *Schistosoma mansoni*, the causative agent of  
99 schistosomiasis, a parasitic disease affecting 200 million people in 78 countries (McManus, 2019).  
100 The interaction of these species is characterized by a phenomenon called compatibility  
101 polymorphism, meaning that some snail phenotypes can be infected by a specific parasite phenotype  
102 while others cannot (Theron et al. 2014). It has been demonstrated that epigenetic alterations are  
103 involved in the *B. glabrata* parasite compatibility phenotype (Knight et al. 2016), even though  
104 contrasting results have been obtained by others (Sullivan 2018, Allan et al. 2020). It remains,  
105 therefore, an open question whether epigenetic mechanisms play a role in the capacity of *B. glabrata*  
106 to produce phenotypic plasticity or variability. DNA methylation machinery components in *B.*  
107 *glabrata* include a maintenance DNMT (*BgDNMT1*), a DNA/tRNA methyltransferase (*BgDNMT2*) and  
108 a methyl-CpG-binding domain protein (*BgMBD2/3*), *BgDNMT1* and *BgDNMT2* being probably  
109 responsible for the 5mC modifications (Fneich et al. 2013, Geyer et al. 2017).

110 *Crassostrea gigas* is a mollusk of commercial importance and its phylogenetic position and life traits  
111 make this bivalve an ideal model to study the physiological, ecological and evolutionary implications  
112 of DNA methylation (Rivière 2014). *In silico* analysis revealed that genes predicted to be  
113 hypermethylated are generally involved in DNA and RNA metabolism and genes predicted to be  
114 sparsely methylated are involved in cell adhesion (Roberts and Gavery 2012a). Similar results were  
115 found in *B. glabrata*: genes predicted to be methylated are associated with housekeeping functions  
116 and genes predicted to be poorly methylated are associated with inducible functions (Fneich et al.  
117 2013). These findings suggest that DNA methylation has regulatory functions in genes implicated in  
118 stress and environmental responses meaning it could contribute to increase phenotypic plasticity in  
119 mollusks and/or produce potentially heritable phenotypic variation (Roberts and Gavery 2012b).

120

121 *Physa acuta* is one of the most widespread freshwater snail invaders (Vinarski 2017) and is an  
122 occasional host of several human trematode diseases, including echinostomiasis and fasciolosis  
123 (Dreyfuss et al. 2002, Kanev 1994). Besides it has been demonstrated to be a bioindicator species for  
124 its sensitivity to environmental contaminants (Müller et al. 2016, Bal, Kumar, and Nugegoda 2017). *P.*  
125 *acuta* has a short generation time that makes it a good model for multigenerational studies (Seeland  
126 et al. 2013). Studies about the impact of toxic compounds in the global DNA methylation of *P. acuta*  
127 and in its phenotypic traits (Bal, Kumar, and Nugegoda 2017) suggest that DNA methylation can play  
128 a role in the phenotypic plasticity of this snail, however, further work is needed to explore this  
129 hypothesis.

130

131 We reasoned that to investigate the role of DNA methylation in mollusks, we must modify its  
132 methylation. We borrowed an approach from cancer biology in which the use of DNMT inhibitors  
133 (DNMTi) has brought considerable advancements in the understanding of DNA methylation  
134 mechanism but also in therapeutic approaches (Gnyszka, Jastrzebski, and Flis 2013, Lopez, Halby, and

135 Arimondo 2016, Geyer et al. 2011(Pechalrieu, Etievant, & Arimondo, 2017). The most used DNMTi in  
136 invertebrates is 5-azacytidine (5-AzaC) (Athanasio et al. 2018, Maharajan et al. 1986, Geyer et al.  
137 2018), nevertheless important advancements in the design of DNMTi have been done in the last  
138 years, notably in decreasing the toxicity and improving the specificity of these compounds (Gros et al.  
139 2012, Pechalrieu et al 2017). Further, 5-AzaC induces unstable and major side-effects, *e. g.* it caused  
140 malformations and apoptosis in the fetal nervous system when administered into pregnant mice  
141 (Ueno et al. 2002). We therefore used to alter DNA methylation in mollusks by using the  
142 commercially available non-covalent nucleoside inhibitor, zebularine (Champion et al., 2010) and  
143 novel generation of non-nucleoside DNMT inhibitors that do not incorporate into DNA and therefore  
144 induce minimal side effects (Erdmann et al. Arimondo, 2015). In addition, we evaluate if DNMTi-  
145 induced DNA methylation modifications are inherited to offspring. For global DNA methylation  
146 screening, we developed a simple, low cost, antibody-based method to measure DNA methylation  
147 levels over large sample numbers and requiring only small amounts of DNA. Our dot blot method and  
148 a commercial ELISA-based kit showed equivalent results. For genome-wide methylation profiling we  
149 used epi-genotyping-by-sequencing method (epiGBS) (van Gurp et al. 2016, Gawehns et al. 2020) and  
150 we compared the results with a previous methylation information obtained by Whole Genome  
151 Bisulfite Sequencing (WGBS) (Adema et al. 2017).

152

153 We tested two types of DNMTi with different mechanisms of action (Supplementary file 1: Figure S1).  
154 We used zebularine, a nucleoside analogue of cytidine that has proven to be an inhibitor of DNA  
155 methylation in human cancer cells (Cheng et al. 2004) but differently from 5-AzaC, it does not form  
156 an irreversible covalent complex with the DNMTs (Champion et al. 2010) and two custom made  
157 compounds (nitroflavanones) that showed *in vitro* inhibition activity against DNMT1 and DNMT3a-c  
158 in human cancer cell lines (Pechalrieu et al. 2020).

159 In summary, our results showed that flavanone Flv1 significantly decreased the 5mC level in the  
160 exposed generation and its progeny, it triggered variation in the morphometric traits in both  
161 generations and it did not show toxic effects. EpiGBS sequencing confirmed the genome-wide effect  
162 caused by Flv1 and allowed us to find Differential Methylated CpG sites (DMCs) between treatment  
163 and control samples. Furthermore, a parental effect was demonstrated by the presence of a  
164 Differential Methylated Region (DMR) in Flv1 exposed snails and its offspring. Flv1-induced  
165 hypomethylation in the BGLTMP010125 *locus* was associated with reduced gene expression. Since  
166 Flv1 inhibitor demonstrated efficiency as DNMTi in *B. glabrata*, it was also tested in the two other  
167 mollusk species: the oyster *C. gigas* and the freshwater snail *P. acuta*, where it triggered also  
168 significant decrease of 5mC, suggesting that Flv1 can be used to modify methylation in other mollusk  
169 species and possibly other invertebrate's taxa. Our results also indicate that induced DNA  
170 hypomethylation is associated with increased phenotypic variance.

171

## 172 **Methods**

### 173 **Ethics statement**

174 *B. glabrata* albino Brazilian strain (BgBRE) was used in this study. *P. acuta* juvenile individuals were  
175 raised in the Centre d'Ecologie Fonctionnelle et Evolutive CEFE UMR 5175 in Montpellier, France. *C.*  
176 *gigas* juveniles' oysters were a generous gift of Bruno Petton from the Marine Mollusks Platform  
177 IFREMER in Bouin, France. *B. glabrata* mollusks were maintained at the IHPE laboratory facilities;  
178 they are kept in aquariums and fed with lettuce *ad libitum*. *C. gigas* and *P. acuta* mollusks were  
179 maintained during the 10 days of drug exposure in the quarantine room at the IHPE laboratory to  
180 avoid contact with the home breeding species (*B. glabrata* strains). The Direction Départementale de  
181 la Cohésion Sociale et de la Protection des Populations (DDSCPP) provided the permit N°C66-136-01  
182 to IHPE for experiments on animals. Housing, breeding, and animal care were done following the  
183 national ethical requirements.

13

14



184 **DNA methyltransferase inhibitor (DNMTi) treatments in *B. glabrata***

185 Three types of DNMT inhibitors were tested in the snail *B. glabrata*, the cytidine analogue zebularine  
186 (Sigma, France, Cat. No. 3690-10-6) and custom-made inhibitors, previously selected for their  
187 inhibitory activity against *hDNMT1* and *hDNMT3-c* (Ceccaldi et al. 2011, , Pechalrieu et al. 2020).

188 The custom-made compounds consist in the active flavanones: Flv1, Flv2, and Flv-neg corresponding  
189 to compounds MLo1507 (3b), DD880 (880) and MLo1607 (19) in Pechalrieu et al. 2020. Stock  
190 solution at 10 mM were made in ultrapure Milli-Q water and aliquoted and stored at -20°C for all  
191 compounds.

192 For each condition, 100 snails *B. glabrata* Brazilian strain (*Bg BRE*) of approximately the same age (8  
193 weeks) and size (5-7 mm) 7mm) were randomly assigned to treatment groups and control groups,  
194 the treatments were done with the drug at a final concentration of 10 µM in 1000 mL of well water in  
195 a plastic container, a single aquarium was made within each treatment. The *Bg BRE* strain is not an  
196 inbred strain, it can show concomitant genetic variability (Carvalho et al. 2001). The water was  
197 replaced once with fresh drug-containing water at the same concentration, the replacement was  
198 performed after 3 days and 22 h. After 10 days of exposure, the drug was removed and replaced by  
199 drug-free water. Snails were then raised in the plastic tank for 70 days, during which different life  
200 history traits were measured. Mortality was measured at days 3, 4, 6, 8 and then each week. The  
201 egg-capsules laid by the snails of the generation F0 were separated each week to raise the F1  
202 generation in another plastic container, the fecundity was reported as a single measure of number of  
203 juveniles and total number of eggs per treatment. At day 70, snails of the generation F0 and F1 were  
204 collected, the shell width, shell height and weight of each snail were recorded to compare  
205 morphometric trait variations between treatments. Finally, snails were stored wrapped in aluminum  
206 sheets individually at -20 °C.

207

208 **Flv1 treatment in *C. gigas* and *P. acuta***

209 Thirty individuals of *P. acuta* and thirty of *C. gigas* were raised as the control groups. Thirty  
210 individuals of *P. acuta* and thirty of *C. gigas* were exposed to the Flv1 inhibitor at a concentration of  
211 10 µM. The water was replaced once with fresh water for *P. acuta* and with filtered sea water for *C.*  
212 *gigas* both containing Flv1 inhibitor at the same concentration, the replacement was done after 3  
213 days and 22 h. After 10 days of exposure, snails and oysters were collected and stored in aluminum  
214 sheets individually at -20°C.

215 **Genomic DNA extraction**

216 Zirconia/Silica beads and the NucleoSpin® Tissue Kit (Macherey-Nagel, Düren, Germany) a method  
217 developed to extract DNA from the Pacific oyster (de Lorgeril et al. 2018) were used for DNA  
218 extraction from whole body without shell of *B. glabrata* (n=300, 30 per treatment), *P. acuta* (n=60)  
219 and *C. gigas* (n=60). Briefly, for the lysis phase, 180 µL of lysis buffer, 25 µL of Proteinase K (20  
220 mg/mL) and 100 µg of zirconia/silica beads (BioSpec, USA, Cat. No. 11079110z) were added to  
221 samples that were submerged in liquid nitrogen and then shaken in a Mixer Mill (Retsch MM400) at a  
222 frequency of 30 Hz for 12 min. Then an incubation in water bath at 56 °C during 1 h 30 was done.

223 After lysis, the NucleoSpin® Tissue Kit protocol was applied according to the manufacturer  
224 instructions. Elution was performed into a final volume of 100 µL elution buffer. The samples were  
225 stored at -20°C. DNA concentrations of all samples were quantified using a Qubit® 2.0 fluorometer  
226 (Invitrogen) and a fluorescence-based Qubit™ dsDNA BR Assay Kit (Invitrogen, Q32853).

227 **DNA methylation screening**

228 Detection and quantification of DNA methylation in genomic DNA were performed by dot blot assays  
229 using an antibody against 5mC. Before large screening, we optimized the dot blot method with DNA  
230 extracted from HeLa cells as a positive control and unmethylated PCR products as negative control.

231 Different concentrations of HeLa cells were spotted to test the sensitivity and linearity of the  
232 method. After standardization of the method, genomic DNA of the control and treated mollusks (100  
233 ng in 5  $\mu$ L per replicate for equal loading) were denatured with 0.3 M NaOH at 42 °C for 10 min and  
234 spotted on nitrocellulose membranes (Hybond®). The membranes were blocked in 5% powdered  
235 milk diluted in 1×TBS containing 0.05% Tween 20 (TBST) for 1 h 30 at room temperature. Then, the  
236 membranes were incubated with a 1:500 dilution ratio of anti-5mC antibody (Abcam, #ab73938) and  
237 5% powdered milk in TBST for 1 h 30, followed by 3×10 washes with TBST and elliptical agitation.  
238 Then incubation with a 1:500 dilution ratio of HRP-conjugated Goat anti-mouse IgG secondary  
239 antibody (ClinicSciences, #AS111772) was done.

240 The antibody mixture was then removed, and the membrane was washed with TBST under elliptical  
241 agitation during 3×10 min. Lecture of the signal was performed using the SuperSignal™ West Pico  
242 Chemiluminescent system (Thermo Fisher Scientific, USA) and the ChemiDoc MP Imaging System.  
243 Finally, the densitometry of the 5mC was analyzed with the software ImageLab5.1. Detailed protocol  
244 of this method is found in our preprint (Luviano et al. 2018).

#### 245 **ELISA-based 5mC quantification**

246 Methylated DNA Quantification Kit (Colorimetric) (Abcam, ab117128) was used to determine global  
247 5mC level in isolated genomic samples of mollusk controls (n=15 for *B. glabrata* and n=10 for *P.*  
248 *acuta* and *C. gigas*) and Flv1 treated (n=15 for *B. glabrata* and n=10 for *P. acuta* and *C. gigas*)  
249 according to manufacturer instructions. To quantify the absolute amount of methylated DNA, a  
250 standard curve was generated plotting the OD values versus the amount of positive control at each  
251 concentration point.

252

253

254 **Statistical analyses**

255 The data of mean spot densitometry provided by the software ImageLab5.1 was normalized by the  
256 DNA amount to obtain a relative measure of the 5mC level. Then, we calculated the 5mC % using the  
257 following equation:

$$258 \text{ 5mC \%} = [\text{sample densitometry/ng}] / [\text{positive control densitometry/ng}] \times \text{Positive control 5mC \%}$$

259 where the positive control densitometry corresponds to  $6.9 \pm 1.2$  per ng of HeLa cells and the  
260 positive control 5mC % corresponds to 2.3% of cytosines methylated in HeLa cells (Diala and Hoffman  
261 1982).

262 Rstudio was used for statistical analysis. When data displayed normal distribution, Student's T test  
263 was used to compare means and when data did not display a normal distribution, then the Wilcoxon  
264 Mann-Whitney test was applied to test significance of differences in means. The survival curves were  
265 compared by a Mantel-Cox test and the fecundity was measured as the number of offspring and the  
266 number of eggs laid by the snails. A contingency table was elaborated with the number of offspring,  
267 the non-hatched eggs and the total of eggs laid, then a Fisher's exact test was done to test for  
268 significant differences between the treatments. PCA analyses with the three morphometric measures  
269 (shell width, shell height and weight) were done to examine variability in all treatments.

270 **Library preparation and high throughput bisulfite sequencing**

271 We used an existing protocol called epiGBS (van Gurp et al. 2016, Gawehns et al. 2020), a reduced  
272 representation bisulfite sequencing method for cost-effective exploration of DNA methylation and  
273 genetic variation designed for multiplexed high-throughput sequencing to maximize sample size  
274 while losing *loci*. epiGBS sequencing was performed with the snails exposed to the DNMTi that  
275 showed the most significant changes in the global 5mC % (Supplementary file 2, Figure S3). Eight  
276 samples per treatment were sequenced from control group, Flv1-treated, and from the progeny of

277 control and the Flv1-treated group. 32 DNA isolated samples were quantified with Qubit fluorometer  
278 with the dsDNA HS Assay Kit (Invitrogen). The concentration was homogenized in all samples to 10  
279 ng/ $\mu$ L in a total volume of 35  $\mu$ L. epiGBS library preparation was applied as described in the step- by-  
280 step most recent protocol (Gawehns et al. 2020). Paired-end sequencing ( $2 \times 150$  bp) using an  
281 Illumina NextSeq™550 instrument at the Bio-Environment NGS Platform at the University of  
282 Perpignan.

### 283 **Bioinformatics epiGBS pipeline**

284 We used the epiGBS2 pipeline (<https://github.com/nioo-knaw/epiGBS2>) to remove PCR duplicates,  
285 and demultiplex samples. We took the filtered and demultiplexed reads from epiGBS2 pipeline to use  
286 another adapted pipeline (Meröndun, Murray, and Shafer 2019). Adapter removing was done using  
287 TrimGalore! V06.5 (Krueger 2012), 30 nucleotides were removed from 3' and 5' end. Single-end  
288 reads were aligned to *B. glabrata* genome v Bglab1 from  
289 <https://www.vectorbase.org/organisms/biomphalaria-glabrata> without scaffolds < 5kb with BSMAP  
290 Mapper (Xi and Li 2009). Then mapped reads were merged and used as input in BSMAP Methylation  
291 Caller to get a tabular file with cytosine and thymine counts that was used as input to calculate  
292 coverage and Frequency of C and T for subsequent analysis.

293 After alignment, we filtered the CpG sites covered by 8 or more reads and pairwise comparisons and  
294 differential methylated analyses were done between control and treated samples in individuals of  
295 the same generation (F0 and F1) using MethylKit (Akalin et al. 2012). The parameters to calculate the  
296 Differentially Methylated Cytosines (DMCs) in MethylKit were q-value < 0.01 and > 15% methylation  
297 difference. The visualization of DMCs was done in Integrative Genomics Viewer (IGV). Reference  
298 transcriptome of *B. glabrata* was uploaded with bigwig files to see the location of DMCs. Genomic  
299 feature annotation was done by visualizing each differential methylated DMCs. Promoter was  
300 arbitrarily defined as the region 2 Kb upstream of transcription start site (TSS).

301 **Bisulfite conversion**

302 300 ng of DNA from 8 control snails and 8 Flv1-treated snails were bisulfite converted as described  
303 previously (Boyd and Zon 2004, Frommer et al. 1992, Grunau, Clark, and Rosenthal 2001). 2 µg of  
304 tRNA from baker's yeast (*S. cerevisiae*) were added to each sample, 3 M NaOH was added to a final  
305 concentration of 0.3 M, and DNA was denatured at 42 °C for 20 min. Then, 240 µL of freshly prepared  
306 bisulfite solution (5.41 g of sodium metabisulfite + 7 mL of distilled water + 0.5 mL of diluted  
307 Hydroquinone [0.022 g/10 mL]) were added to the denatured DNA samples and incubated in the  
308 dark during 4 h at 55 °C. After that, 200 µL of distilled water were added to the samples, and the total  
309 volume was transferred to an Amicon column (UFC501024, Millipore), and centrifugation was done  
310 at 12 000 g during 5 min. The column was washed 3 times with 350 µL of distilled water and  
311 centrifugation at 12 000 g during 5 min was done each time. Following this, 350 µL of 0.1 M NaOH  
312 was added to the DNA in the Amicon column, centrifuged at 12 000 g during 5 min, subsequently 350  
313 µL of distilled water were added and a centrifugation at 12 000 g for 5 min was done. 50 µL of 10 mM  
314 TRIS/Cl pH 7.5-8.0 was added to the DNA in the Amicon column and it has been incubated at room  
315 temperature during 5 min. Finally, the tube was inverted, and the DNA was collected by  
316 centrifugation at 1000 g for 3 min. DNA was stocked at -80 °C.

317 **Nested PCR amplification of bisulfite converted DNA**

318 Primers were designed for PCR amplification in a CpG rich region of the first intron of the  
319 BGLTMP010125 gene using MethPrimer (Li and Dahiya 2002). The external primers (forward  
320 ATTGTGTTTTATTTTGATGGTTATGATA and reverse CCCCAAACTTACAAAACCTTAC) were used to  
321 amplify a region spanning 861 bp in the BGLTMP010125 gene (Scaffold 4692: 13866-14343). The  
322 internal primers used in the nested PCR were the forward primer AGTTTTTTTTATTTGTATGTAGAGT  
323 and the reverse primer ATCCTTTCAAAAACAAATCATATATC; that amplify an amplicon of 565 bp. The  
324 initial PCR amplification was performed using 1 µL of the bisulfite converted gDNA samples as

325 templates with external primer set as follows: 94 °C for 2 min, 5 cycles of 94 °C for 1 min, 50 °C for 2  
326 min and 72 °C for 3 min, followed by 30 cycles of 94 °C for 30 secs, 50 °C for 2 min and 72 °C for 1:30  
327 min and finally 72 °C for 10 min. The nested PCR was performed on a 10-fold dilution of the first PCR  
328 product using the internal primer set in the same conditions as for the first PCR. PCR products were  
329 separated by electrophoresis through 2% agarose gels to check for the specific amplification of each  
330 target gene. PCR products were sequenced by Sanger sequencing (Genoscreen, Lille, France).  
331 Sequence chromatograms were analysed as previously described (Jiang et al. 2010) to measure T-  
332 peaks heights for unmethylated cytosines converted to thymines, and C-peaks heights for  
333 methylated cytosines, providing an estimate for the degree of methylation.

#### 334 **Dual DNA and RNA extraction and RT-qPCR**

335 DNA and RNA were extracted from the same samples (n=8 per treatment) with TRIzol reagent (Sigma  
336 Life Science) according to manufacturer's instructions. DNA was subsequently bisulfite converted as  
337 described previously and RNA was reverse transcribed to first strand cDNA using Maxima H Minus  
338 First Strand cDNA Synthesis Kit with dsDNase to remove contaminating genomic DNA and following  
339 manufacturer's instructions (Cat. Num. K1682, ThermoFisher, Scientific). Real-time RT-qPCR analyses  
340 were performed using the LightCycler 480 System (Roche) in a 10 µL final volume comprising 5 µL of  
341 No Rox SYBR Master Mix blue dTTP (Takyon), 1.75 µL of ultrapure MilliQ water, and 1 µL of each  
342 primer at a concentration of 1 µM. The primers used for the RT-qPCR are shown in the Table 1. Two  
343 housekeeping genes were used to normalize the results, the 28S ribosomal protein gene and the  
344 αTubulin protein gene, the primers efficiencies were previously evaluated by amplifying four  
345 different dilutions of each couple of primers at the RT reaction (1:1, 1:10; 1:100 and 1:1000), a  
346 standard curve was generated and the efficiency was calculated with the equation (Efficiency of the  
347 amplification=  $10^{(1/-\text{slope})}$ , as earlier described (Jozefczuk and Adjaye 2011). The cycling program was:  
348 denaturation step at 95 °C for 2 min, 40 cycles of amplification (denaturation at 95 °C for 10 secs,

349 annealing at 58 °C for 20 secs, and elongation at 72°C for 30 secs), with a final elongation step at 72°C  
 350 for 5 min. For each reaction, the cycle threshold (Ct) was determined using the second derivative  
 351 method of the LightCycler 480 Software release 1.5.0 (Roche). Reactions without RT served as  
 352 negative control for each sample (in duplicate) to exclude amplification of DNA. None of these  
 353 negative RT reactions amplified the target. All PCR experiments were performed in duplicates  
 354 (technical replicates). The mean Ct value of each reaction was calculated and the  $2^{-\Delta\Delta CT}$  method was  
 355 applied to calculate relative gene expression, the geometric mean of the Ct values of two  
 356 housekeeping genes (28S and  $\alpha$ -Tubulin) were used to normalize gene expression. Corrected melting  
 357 curves were checked using the Tm-calling method of the LightCycler 480 Software release 1.5.0.

358 **TABLE 1.** *Biomphalaria glabrata* gene-specific primers used to amplified gene fragments used in the  
 359 RT-qPCR.

Gene	Primer Sequence	Amplicon lenght	Primer efficiency
28S ribosomal protein	F : GCTGGCACGACCGCTCCTTT	100 bp	2.01
	R : TTTGAACCTCGCGACCCGGC		
$\alpha$ -Tubulin	F : CGACATCTGCCGCGTAACCT	112 bp	2.04
	R : GGCGCCATCAAACCTGAGGGA		
BGLTMP010125-RA:	F : TTGCTGTGACTGTCAGTGTC	95 bp	1.90
	R : TAGACTCAATGGACGGTGGAC		

360

### 361 Nuclear fraction extraction

362 Nuclear fractions were prepared by collecting *Bge* cells (the embryonic cell line of our model *B.*  
 363 *glabrata*) by centrifugation, then cell pellet was lysed with a dounce homogenizer (7 mL) for 10 min  
 364 at room temperature with cold 10 mM HEPES pH 7.7, 10 mM KCl, 0.1 mM EDTA, 1 mM DTT, and 0.4%  
 365 IGEPAL CA-630 in the presence of protease inhibitors. The lysed cells were centrifuged at 15,000 x g  
 366 for 3 min and the soluble fractions removed. The pellet was resuspended in 20 mM HEPES pH 7.7, 0.4  
 367 M NaCl, 10% glycerol, 1 mM DTT in the presence of protease inhibitors by vortexing for 2 h at 4 °C,  
 368 followed by centrifugation at 15,000 x g (5 min, 4 °C) to provide the nuclear fractions (supernatant)



369 and a membrane pellet. The nuclear fractions were quantified with the 2D Quant Kit (GE Healthcare  
370 Life Sciences, USA) and then stored at -80 °C until use.

### 371 **Chemical stability measurement**

372 The flavanone compounds stability was measured by High Performance Liquid Chromatography  
373 (HPLC) by the method described in Pechalrieu *et al.*, 2020. HPLC analysis were done using an X-terra  
374 column (100 × 4.6 mm; 5 µm) with 1 mL/min flow and the following gradient: H<sub>2</sub>O acetonitrile 95:5  
375 for 2 min then up to 0:100 in 10 min and maintained at 0:100 for 2 min with H<sub>2</sub>O and acetonitrile  
376 containing 0.1% of trifluoroacetic acid. First, flavanone compounds (Flv1, Flv2 and Flv-neg) were  
377 injected in solution at 100 µM in 100% DMSO to check its purity. Then 50 µL of solution at 10 µM of  
378 tested compound was prepared by dilution in DNMT3A-c enzyme buffer (Hepes 20 mM pH 7.2, KCl  
379 50 mM, EDTA 1 mM final concentration), in freshwater used in the aquariums of *B. glabrata* or in  
380 filtered sea water used in the aquariums of *C. gigas*. The percentages of remaining compound were  
381 determined with the area of the corresponding HPLC peak on the 250 nm chromatogram.

### 382 **DNMT inhibition assays**

383 Compound activities were determined with a fluorescence-based assay (Ceccaldi *et al.* 2011). In brief,  
384 a double-strand DNA with a unique CpG site overlaying an endonuclease restriction site for  
385 methylation-sensitive enzyme was used. This oligonucleotide comprises a 6-carboxyfluorescein (6-  
386 FAM) at one end and biotin on the other end allowing immobilization into a 384-well plate  
387 (PerkinElmer) pre-coated with avidin. Compounds to be evaluated and SAM as methyl donor were  
388 added followed by DNMT3A-c to start the methylation reaction, which was prolonged 1 h at 37 °C.  
389 After several washing, with PBS tween (0.05%) containing NaCl (0.5 M) and PBS tween (0.05%).  
390 Restriction step was performed with HpyCH4IV (New England, BioLabs) to hand on only the specific  
391 fluorescence signal. Fluorescence was quantified on a spectrofluorometer SAFAS FLX-Xenius.

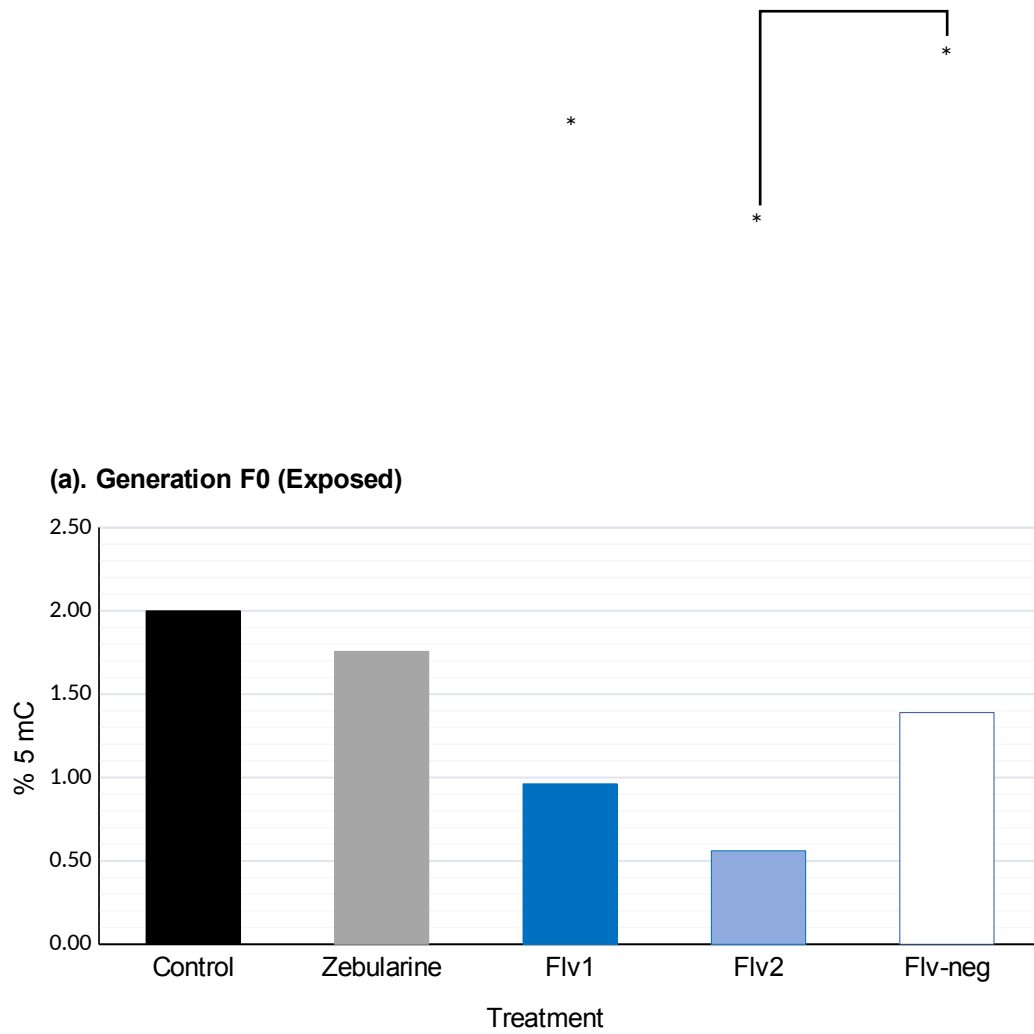
392 Methylation activities are defined as  $[(X_{\text{meth}}-X_{\text{restri}})/(X_{\text{DNA}}-X_{\text{restri}})] \times 100$ , where  $X_{\text{meth}}$ ,  $X_{\text{restri}}$  and  $X_{\text{DNA}}$  are  
393 respectively the fluorescence signals of the compound methylation, restriction and DNA controls.

## 394 **Results**

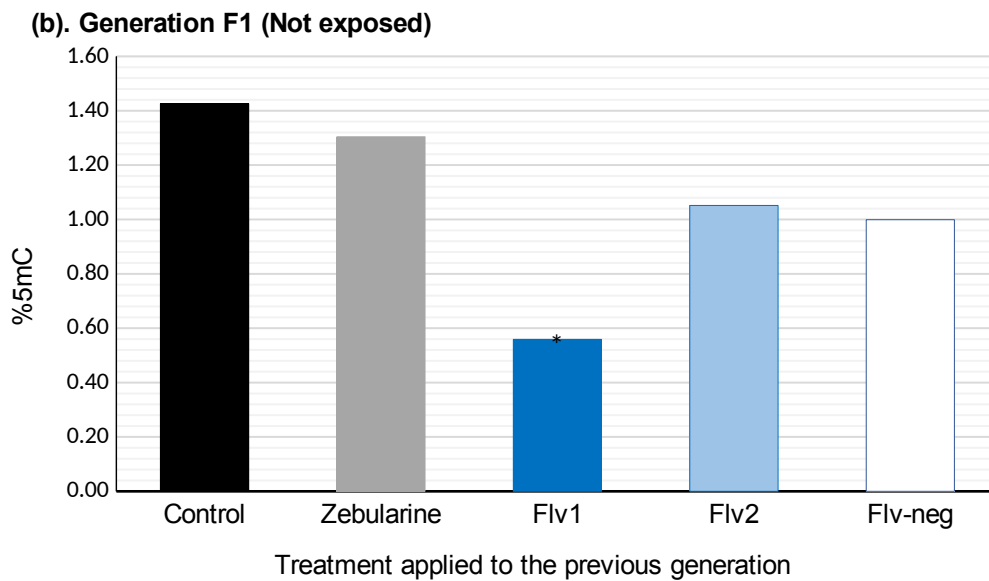
### 395 **New DNMTi influence global DNA methylation *in vivo* over two consecutive generations** 396 **(multigenerational effect)**

397 Using a newly developed population epigenetics screening method that delivered results comparably  
398 to ELISA (Supplementary file 2, Figure S4 and S5) but at much lower costs (Luviano et al. 2018) we  
399 showed that, in the F0 generation, zebularine did not produce a statistically significant difference in  
400 5mC % compared to the control group (W=383, p=0.32). However, 5mC % was significantly different  
401 in the groups treated with Flv1 (W=365 p<0.0001) and Flv2 (W=445, p<0.0001) compared to control.  
402 The reduction in 5mC % between control (2%) and Flv1 (0.96%) was 2-fold (Figure 1a). Unlike Flv1,  
403 Flv2 showed a significant difference compared to the inactive flavanone Flv-neg (W=361, p<0.0001).

404 In the F1 generation, offspring snails of the Flv1 exposed generation presented a significantly lower  
405 5mC % (W=713, p<0.0001) than the control group (Figure 1b).



406



407

408 **FIGURE 1.** 5mC % of *B. glabrata* snails upon DNMTi treatments at a concentration of 10  $\mu$ M, error  
 409 bars represent SD, n=30 per treatment. (a) 5mC % in the F0 generation (exposed), black bar for  
 410 control, grey bar for zebularine, blue bars represent the flavanone inhibitors (blue bar for Flv1 and  
 411 light blue bar for Flv2) and the white bar with blue outline represent the inactive Flv-neg. (b) 5mC %  
 412 in the non-exposed F1 generation. Compounds are the ones used in F0. Mann-Whitney Wilcoxon test  
 413 was applied, if not otherwise indicated, between treatment and control significant differences are  
 414 marked as \* for  $p < 0.0001$ . 5mC ng was normalized to the 5mC global percentage present in the  
 415 genome of *B. glabrata*.

416 **Flv1 blocks DNMT activity *in vitro***

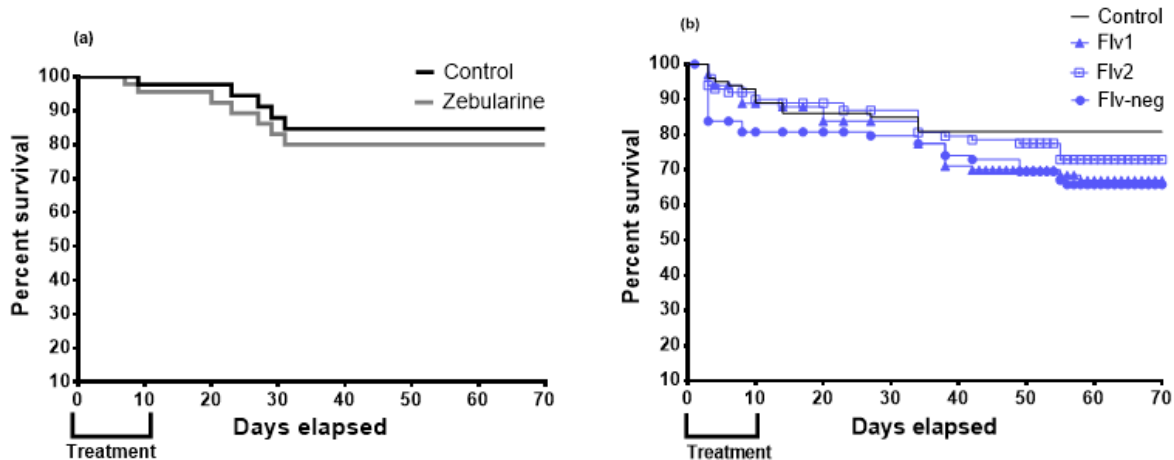
417 After having firmly established that Flv1 inhibits DNA methylation *in vivo* in *B. glabrata* we wondered  
 418 if this effect was due to a direct action on DNMT or whether it was indirect by influencing upstream  
 419 pathways. To verify this, we extracted soluble nuclear proteins from *Bge* cells and performed an *in*  
 420 *vitro* enzyme inhibition assay. We showed that methylation activity of *Bge* nuclear protein extract  
 421 was inhibited by 55% and 78% after treatment with 32  $\mu$ M and 100  $\mu$ M of Flv1, respectively  
 422 (Supplementary data 1, Figure S2).

37

38

423 **DNMTi influence survival, fecundity and morphometric traits**

424 Since our findings had clearly indicated that Flv1 had an *in-vivo* and *in-vitro* demethylating activity *i.e.*  
425 probably due to a direct effect on the DNMT we wondered if this epimutagenic activity had  
426 phenotypic consequences. Therefore, we measured survival, fecundity and morphometric traits in  
427 the DNMT-treated snails. We used as pharmacological reference molecule zebularine. Zebularine  
428 induced the lowest mortality with no significant difference compared to control group (Mantel-Cox  
429 test  $\chi^2=0.3$ ,  $p=0.56$ ). This compound followed a similar trend as the control and the snail final survival  
430 rate reached 80% compared to 84% in the control. (Figure 2a). The mollusks treated with Flv1, Flv2  
431 and the inactive Flv-neg had a survival rate of 68%, 73%, and 69%, respectively (Figure 2b), and none  
432 of these rates were statistically different compared to the control group ( $\chi^2=3.5$ ,  $p=0.06$  for Flv1,  
433  $\chi^2=1.16$ ,  $p=0.2$  for Flv2 and  $\chi^2=5.9$ ,  $p=0.1$  for Flv-neg).



434

435 **FIGURE 2.** Kaplan-Meier survival curves upon treatment with the two types of DNMTi. (a) Cytidine-  
436 analogue zebularine (grey line). (b) Flavanones Flv1 (blue line with triangles) and Flv2 (blue line with  
437 squares) and their inactive derivative Flv-neg (blue line with circles).

438 The fecundity of snails was affected by the treatment with Flv2. With zebularine the number of the  
439 offspring was significantly lower than the control group (Fisher's exact test,  $p<0.0001$ ) and the

440 number of eggs was very high compared to the other treatments (Table 2). Mollusks treated with  
 441 Flv2 presented a low number of offspring (n=20) and it was significantly different compared to  
 442 control group (p=0.004); the treatments with Flv1 and Flv-neg showed no significant difference in the  
 443 number of offspring against control group.

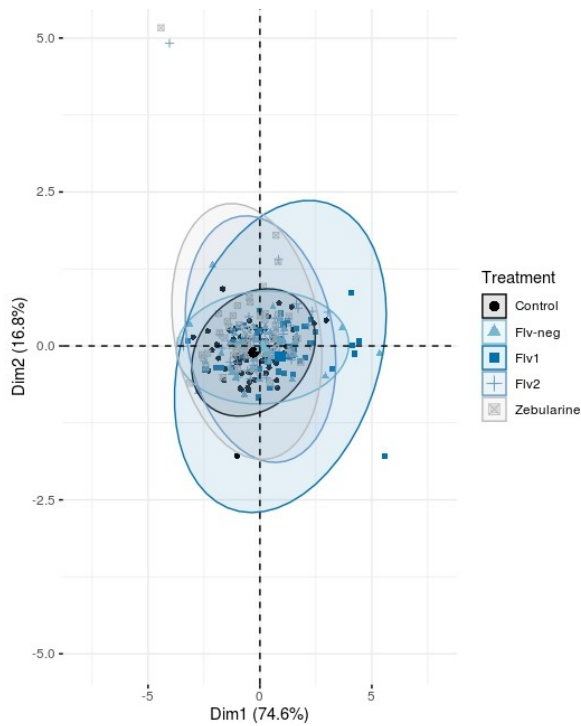
444 **TABLE 2.** Contingency table of fecundity of the snails exposed to different DNMTi. Total number of  
 445 laid eggs (first row), number of non-hatched eggs (second row) and number of offspring snails (third  
 446 row). Fisher's exact test was applied, significant differences with control group are marked with \* for  
 447 p<0.005 and \*\* for p<0.0005.

	Control	Flv1	Flv2	Flv-neg	Zebularine
<i>Total number of laid eggs</i>	191	183	199	188	326
<i>Number of non-hatched eggs</i>	152	147	179	147	301
<i>Number of offspring</i>	39	36	20*	41	25**

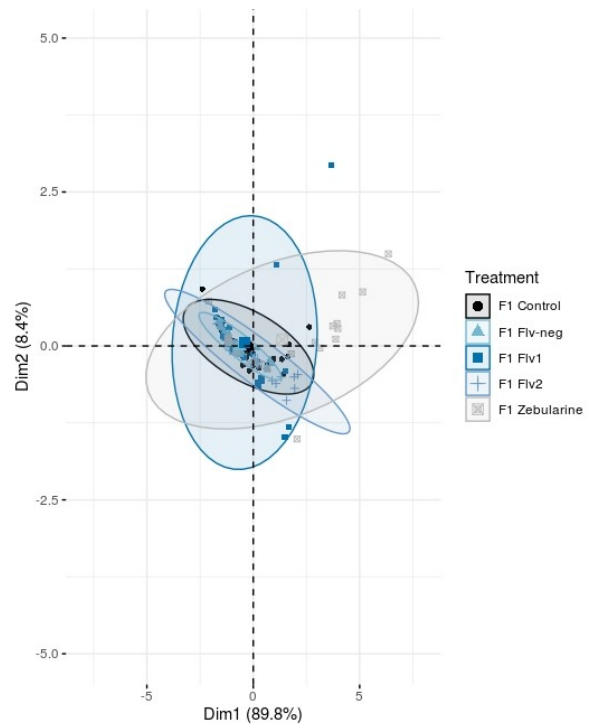
448

449 To visualize the variation of morphometric traits induced by DNMTi treatment in the F0 generation  
 450 and in its respective offspring, we performed PCA with three morphometric measures. Flv1  
 451 treatment induced the largest variance (the highest range of values in the axis of the PCA plot) in  
 452 both the F0 and F1 generations (Figure 3). In other words, the inhibition of DNMT activity by Flv1 led  
 453 to a decrease of global DNA methylation and resulted in a higher diversity of morphometric traits in  
 454 the Flv1-treated population and its offspring (Figure 3 e-f).

(a) PCA morphometric traits F0 generation

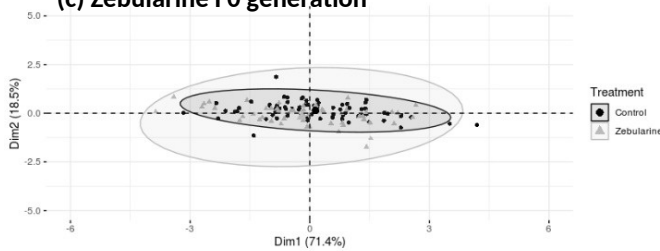


(b) PCA morphometric traits F1 generation

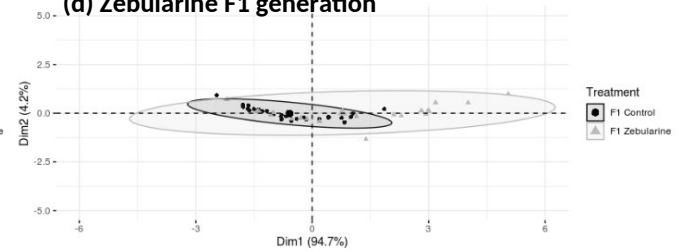


455

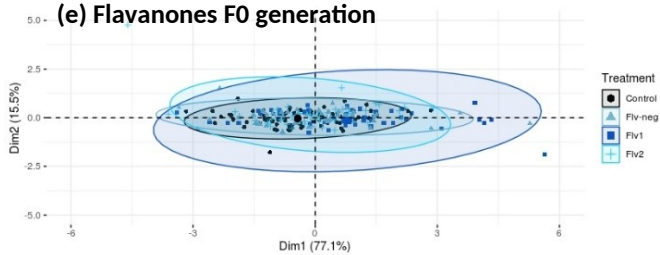
(c) Zebularine F0 generation



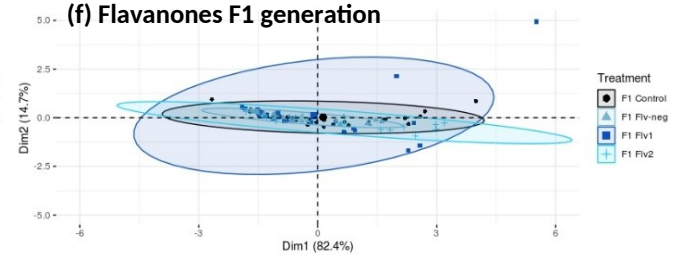
(d) Zebularine F1 generation



(e) Flavanones F0 generation



(f) Flavanones F1 generation



456

457 **FIGURE 3.** PCA of morphometric traits of all treatments of F0 (a) and F1 generation (b). PCA analyses  
458 splitted by treatment, (c) PCA of morphometric traits after zebularine treatment and (d) its offspring  
459 (e) PCA of morphometric traits of snails exposed to flavanone derivatives F0 generation and (f) the  
460 non-exposed F1 generation. The confidence ellipses show a confidence interval of 95%. The axis 1  
461 includes the three morphometric measures (shell width, height and weight) and the axis 2 include  
462 shell width and height.

43

44

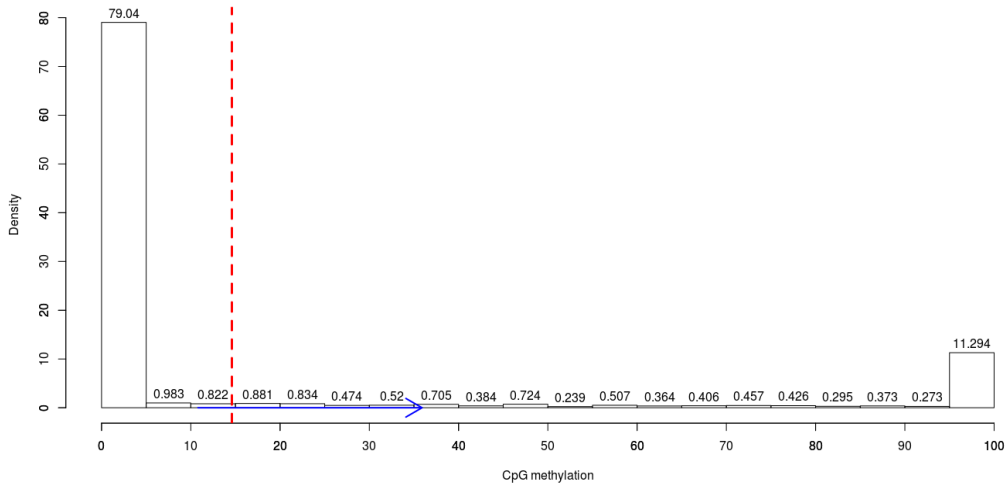
463 **epiGBS reduces sequencing effort roughly 10x but allows for reliable evaluation of global 5mC level**  
464 **and identification of differentially methylated sites and regions**

465 To obtain a clearer picture of where hypomethylation occurred in the epigenomes of the DNMTi  
466 exposed populations and their offspring we adapted a reduced representation technique that was  
467 originally developed for mosaic methylation of plants: epigenotyping by sequencing (epiGBS). Since it  
468 was the first time epiGBS was used on mollusks, we first had to make sure that it delivers reliable  
469 results here. We used our previously obtained WGBS data (Adema et al. 2017) to compare the WGBS  
470 to epiGBS results on *B. glabrata*. We reanalyzed the WGBS data with updated pipeline analysis and  
471 generated a new reference methylome of *B. glabrata*. Using the BSMAP Mapper, 46.2% of reads  
472 mapped unambiguously to the *B. glabrata* reference genome. Paired-end sequencing of the 32  
473 pooled epiGBS libraries (8 per treatment) resulted in a total of 140,751,495 filtered and  
474 demultiplexed reads. After quality control and alignment, an average of 34% of unique reads per  
475 sample mapped to the *B. glabrata* reference genome using BSMAP Mapper (Supplementary file 1,  
476 Table S1). After methylation calling, 6 samples per treatment with CpG sites covered by  $\geq 8$  reads  
477 were retained for further analysis, the removed samples showed very low number of CpG sites  
478 ( $< 4200$ ). After filtering; we obtained an average of 47,715  $\pm$  31,774 methylated CpG methylation  
479 positions per sample (Supplementary file 1, Table S1).

480 To analyze the distribution of methylated CpG over the entire genome we represented its frequency  
481 distribution. We found a characteristic distribution of two peaks for both WGBS and epiGBS  
482 indicating the majority of the CpG sites being either unmethylated or completely methylated, as  
483 expected for a species that displays a mosaic distribution type of DNA methylation pattern (Figure 4  
484 a-c). The peak of methylated CpG sites was higher in the epiGBS sequencing results compared to  
485 WGBS, but mean CpG methylation values and confidence interval (CI) of 95% were highly similar in  
486 both methods (Figure 4 a-c).

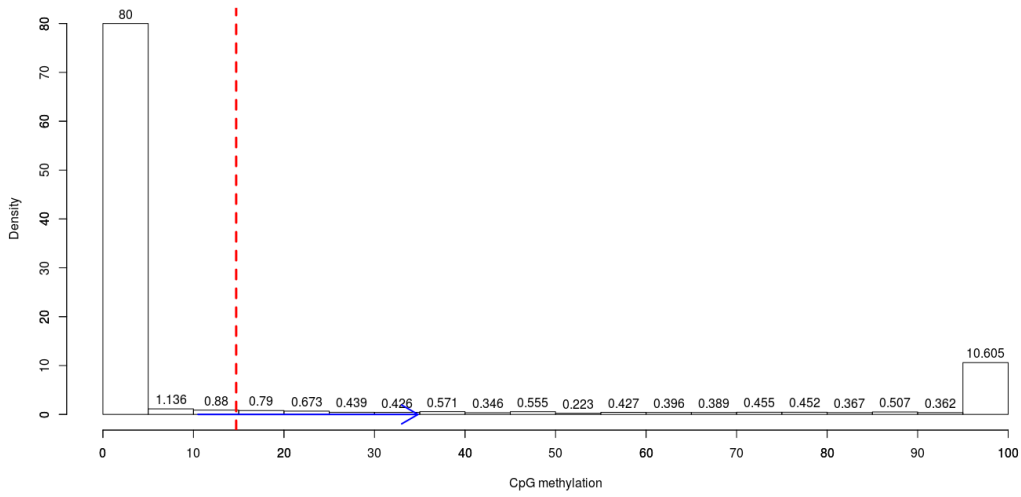


(a) Histogram of CpG methylation F0 Controls epiGBS



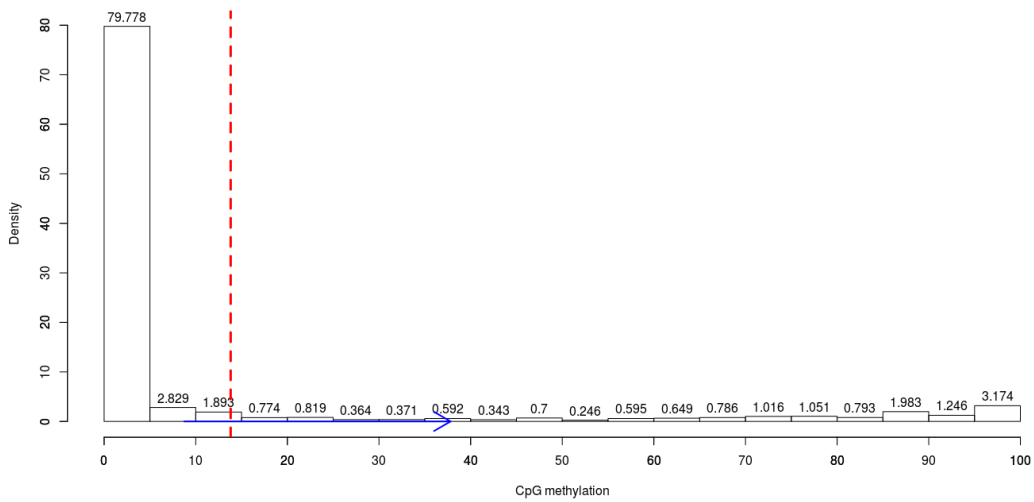
487

(b) Histogram of CpG methylation F1 Controls epiGBS



488

(c) Histogram of CpG methylation WGBS



489

47

48

490 **FIGURE 4.** Histograms of CpG methylation distribution, (a) histogram of F0-control epiGBS libraries  
491 (b) histogram of F1-control epiGBS libraries and (c) histogram of WGBS library. The abscissa  
492 represents the CpG methylation % (0-100) and the ordinate showed the density of CpG positions. The  
493 dashed red line indicates the mean CpG methylation value and the blue arrow indicates the  
494 confidence interval (CI) of 95%.

495 A direct comparison was done to examine the data obtained for CpG methylation from epiGBS library  
496 versus WGBS (Supplementary file 1, Table S1). We chose the best covered control samples from each  
497 generation of epiGBS libraries to compare them with WGBS. WGBS data had a higher mapping  
498 efficiency than epiGBS (46.2% compared to 32.8%). The number of CpG sites with a minimum read  
499 coverage of 8x was of 34,646 and 63,892 for epiGBS libraries and 4,061,906 for WGBS. epiGBS  
500 represents 0.8% (epiGBS F0) and 1.6% (epiGBS F1) of the CpG sites covered by WGBS. However, the  
501 average levels of CpG methylation percentage were very similar between both methods (Table 3).

502

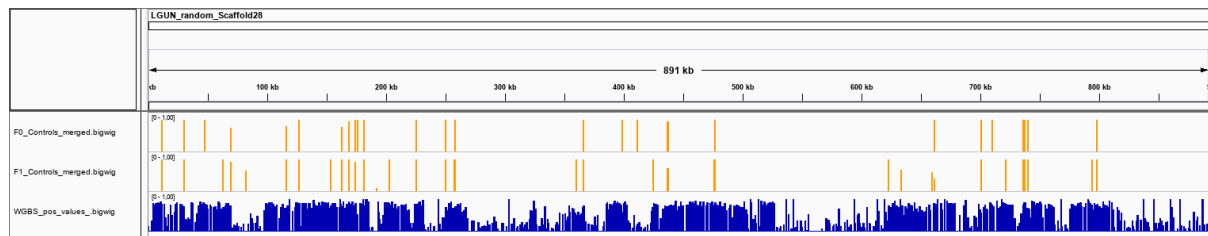
503 **TABLE 3.** Mapping efficiencies, CpG coverage and average genome-wide methylation levels resulting  
 504 from epiGBS and WGBS libraries.

Samples	Mapping efficiency%	Sequence reads	Total no. CpGs	CpGs $\geq$ 8x coverage	Methylated CpG sites	Methylated CpG %
epiGBS F0	34.3	707 010	95 369	34 646	7 621	22.0
epiGBS F1	34.5	1 299 293	180 852	63 892	13 982	21.9
WGBS	46.5	152 842 929	17 493 207	4 061 906	855 624	21.1

505

506 To evaluate concordance of epiGBS and WGBS, a correlation was done with the methylation values  
 507 of CpG positions covered by both methods. A high correlation was found between WGBS and epiGBS,  
 508 Spearman correlation,  $R=0.74$ ,  $p<2.2e^{-16}$ . We also visualized the CpG methylation profile of epiGBS  
 509 samples compared to WGBS in IGV in a wide-ranging Scaffold. Visual inspection showed that both  
 510 epiGBS libraries of F0 and F1-controls have similar methylation profiles (Figure 5 yellow bars) while,  
 511 naturally, epiGBS results represent a small fraction of the information found with WGBS (Figure 5,  
 512 blue bars).

513

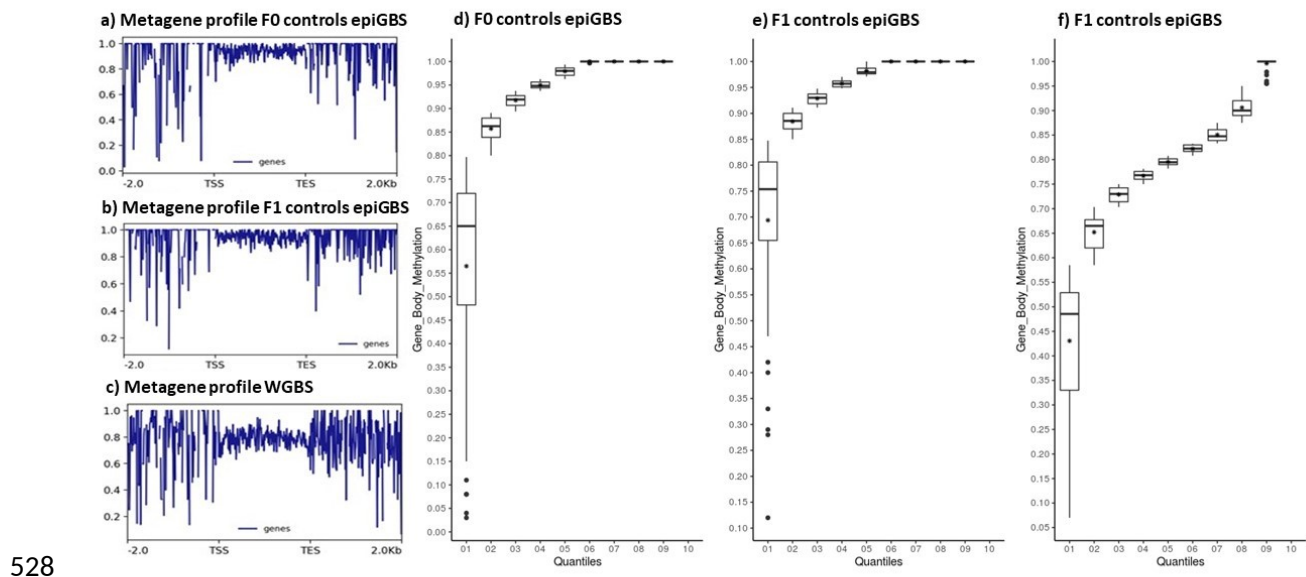


514 **FIGURE 5.** Screenshot of IGV of the region LGUN\_random\_Scaffold28: 1-800 Kb, that showed the  
 515 regions covered by epiGBS libraries (in yellow) versus the regions covered by WGBS library (blue).

516 We then produced the CpG methylation metagene profiles across gene bodies from 2kb upstream of  
 517 the transcription start sites (TSS) and 2kb downstream of the transcription end sites (TES). The CpG  
 518 sites used for these profiles were those covered by both methods. We found that CpG methylation  
 519 levels remained a plateau after TSS and along the gene bodies and then showed a high range of

520 methylation before TSS and after TES in both methods. The range of GBM levels were different in  
521 epiGBS libraries (0.9-1) (Figure 6a-b) than in WGBS (0.7-0.9) (Figure 6c).

522 The quantile distribution of GBM was different between epiGBS and WGBS. In the epiGBS libraries of  
523 F0 and F1 controls, the highest quantile is the first one and comprises CpG values of 0.15-0.80 and  
524 0.47-0.85 (Figure 6d-e). In the WGBS library, the highest quantile is also the first one but comprises  
525 values of 0.07 to 0.58 (Figure 6f). When all CpG sites covered by WGBS are compared to epiGBS  
526 libraries, the metagene profiles and the quantiles distribution are, as expected, more marked  
527 (Supplementary file 2 Figure S6).



528  
529 **FIGURE 6.** CpG methylation ratio profile across the bodies of genes and quantiles distribution of  
530 epiGBS and WGBS libraries. (a) Metagene profile of CpG methylation ratio of F0 control epiGBS  
531 libraries, (b) F1-control epiGBS libraries and (c) WGBS library. -2.0 kb indicates the upstream 2,000  
532 bp of TSS, and 2.0 kb indicates the downstream 2,000 bp of TES. Quantiles (deciles) distribution of  
533 Gene body methylation of (d) F0-control epiGBS (e) F1-control epiGBS and (f) WGBS.

534 The global distribution of CpG methylation sites displayed a two-peak histogram in all epiGBS  
535 samples, with most of the CpG sites being either unmethylated or completely methylated. The

536 percentage of CpG sites which displayed no methylation or complete methylation for each sample  
 537 are indicated in Table 4.

538 In summary, epiGBS mirrors WGBS on a global scale but has necessarily a lower resolution (at our  
 539 sequencing depth about 1% of the CpG sites are captured) and it also has a slight bias towards  
 540 methylated regions of the epigenome.

541 **TABLE 4.** Percentage of CpG methylation sites which display an unmethylated or complete  
 542 methylated pattern.

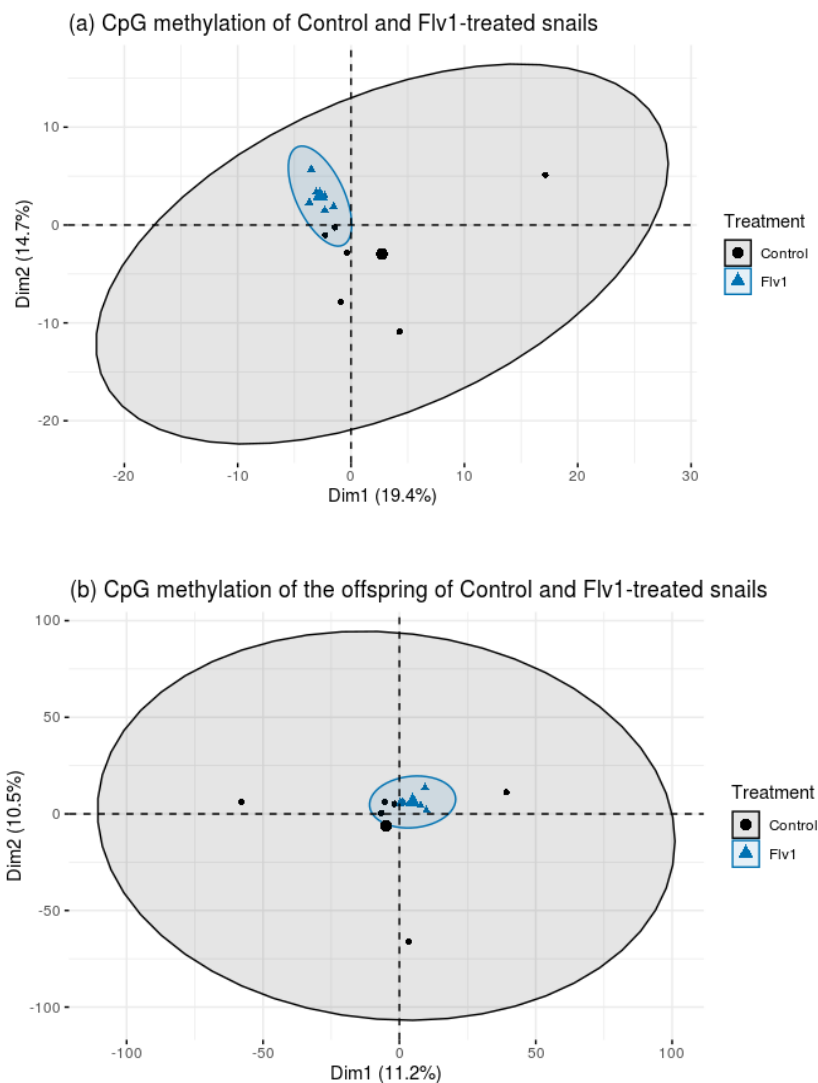
Generation F0			Generation F1		
Samples	CpG methylation frequency		Samples	CpG methylation frequency	
	Unmethylated %	Completely methylated %		Unmethylated %	Completely methylated %
Control 1	78	9.9	F1-control 1	81.2	13.6
Control 2	77.6	10.4	F1-control 2	78.6	9.7
Control 3	79.7	10.5	F1-control 3	82.4	13.5
Control 4	79.6	12.5	F1-control 4	82.4	13.5
Control 5	77.6	11.7	F1-control 5	81.5	12.5
Control 6	79.2	11	F1-control 6	82.3	12.6
Flv1-1	80.9	9.4	F1-Flv1-1	80.4	10.6
Flv1-2	77.1	8.7	F1-Flv1-2	80.9	10.8
Flv1-3	80.4	11.9	F1-Flv1-3	81	10.6
Flv1-4	82	13.4	F1-Flv1-4	82.9	11.8
Flv1-5	80.9	12.2	F1-Flv1-5	81.2	11.1
Flv1-6	81.9	12.7	F1-Flv1-6	81.7	11.2

543

544 **epiGBS corroborates multigenerational hypomethylation by Flv1**

545 We considered epiGBS a reliable method that allows for epigenome-wide analysis of DNA  
 546 methylation changes in populations at reasonable costs and we used it to capture regional  
 547 methylation differences in Flv1 -treated samples. The mean percentage of CpG methylation was 15.8  
 548  $\pm 0.8$  % in control snails and 13.5  $\pm 0.6$  % in Flv1-exposed snails, 13.5  $\pm 0.3$  % in offspring of control  
 549 snails and 13.1  $\pm 0.1$  % in the offspring of Flv1-exposed snails. There was significant difference in  
 550 global percentage of CpG methylation between control and Flv1-exposed snails ( $t= 6.0$ ,  $df= 9.4$ ,  $p=$   
 551 0.0001) and significant difference was also found in their offspring ( $t= 3.0$ ,  $df= 6.0$ ,  $p=0.023$ ).

552 PCA analysis of CpG methylation was performed on controls and Flv1-treated samples (Figure 7).  
553 Interestingly, Flv1-treated samples clustered tightly, while control samples were spread out (Figure  
554 7a). PCA analysis of CpG methylation in F1 generation showed the same tendency, F1-Flv1 samples  
555 were grouped and F1-control samples dispersed (Figure 7b). PCA of both generations displayed the  
556 same pattern, indicating an impact in the CpG methylation at the genome-wide level and a decrease  
557 of CpG methylation variability/diversity in both generations.



558

559

560 **FIGURE 7.** PCA of CpG methylation of the Flv1-treated and control groups in F0 generation (a) and in  
561 its offspring (b). The ellipses represent the 95% confidence interval.

57

29

58

562 **One out of eight of Flv1-induced hypomethylated DMR is heritable**

563 Differential Methylated CpG sites (DMCs) were analyzed between control and Flv1-treatment in both  
 564 generations. We found multiple DMCs concentrated in DMRs, one DMR consists in 2 or more DMCs  
 565 found in the same genomic region (within 3.5 Kb). We found 25 DMCs in the F0 generation between  
 566 control and Flv1-exposed samples, comprising 23 hypomethylated CpG sites and two  
 567 hypermethylated CpG sites (Table 5). The higher content in hypomethylated CpG sites further  
 568 confirmed the genome-wide effect of the Flv1 inhibitor. Interestingly, these DMCs are not isolated  
 569 and rather concentrated in some closed regions: the 25 DMCs comprise eight DMRs (Supplementary  
 570 file 1, Table S2).

571 **Table 5.** DMCs in Flv1-treated and control group for each generation. The parameters to calculate  
 572 the DMCs were q-value < 0.01 and > 15% methylation difference.

Treatment	Generation	Total DMCs	Total DMRs	Hypomethylated DMCs	Hypomethylated DMRs	Hypermethylated DMCs	Hypermethylated DMRs
Flv1	F0	25	8	23	6	2	1
Flv1	F1	325	51	203	38	120	13
Flv1	F0 and F1	6	1	6	1	0	0

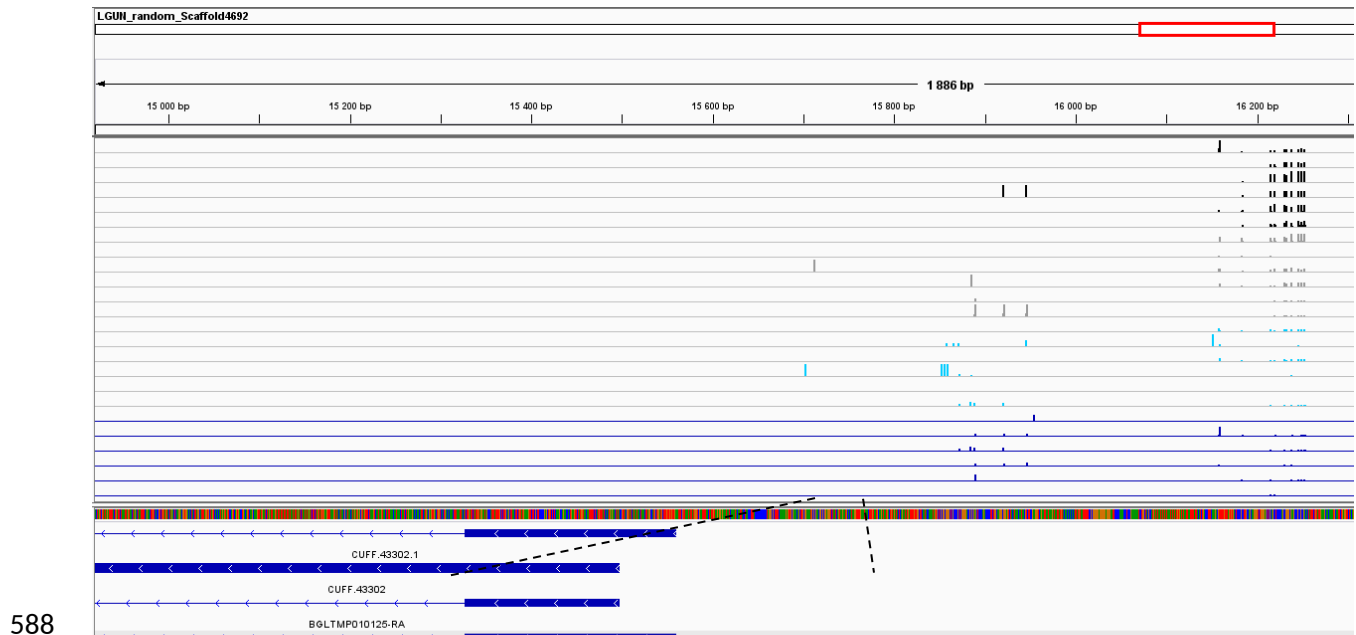
573

574 In the generation F1, 323 DMCs were found between F1-control and F1-Flv1 samples, 203  
 575 hypomethylated and 120 hypermethylated (Table 5). The majority of hypomethylated DMCs  
 576 demonstrates a hypomethylated genome wide effect. 325 DMCs represent a considerably higher  
 577 amount of DMCs than in the generation F0. The context of each DMC was examined, the majority of  
 578 hypomethylated DMCs were found in the intergenic region (42.8%), 19.7% in the promoter region,  
 579 28.1% in introns and 9.4% in exons. In the case of hypermethylated DMCs, 32.5% were found in the  
 580 intergenic region, 11.7% in the promoter region, 30% in introns and 25.8% in exons (Supplementary  
 581 file 1, Table S3). The 203 hypomethylated DMCs are concentrated in 38 DMRs and the 120  
 582 hypermethylated DMCs are concentrated in 13 DMRs.

583 Six DMCs were common between both generations, being hypomethylated, five of these DMCs were  
584 found in one DMR, which was visualized in the Integrative Genomics Viewer (IGV) using the *B.*  
585 *glabrata* genome (Assembly GCA\_000457365.1) and the reference transcriptome for annotation  
586 (Figure 8). The DMR is close to transcript BGLTMP010125.

587





588

589

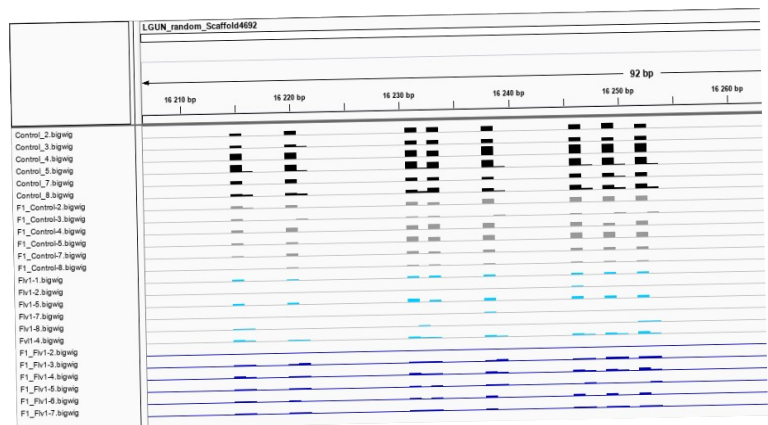
590

591

592

593

594



595 **Figure 8.** IGV screenshot of the LGUN\_random\_scaffold4962:16175-16266 of *B. glabrata* genome

596 assembly (GCA\_000457365.1). Each bar indicates the position of a methylated CpG site for the

597 different samples: F0-control F0 (black), F1-control (gray), Flv1-treated samples (light blue) and its

598 offspring (dark blue). Hypomethylated DMCs have been detected in this region and are in common

599 between F0 and F1 generation.

600

601

63

64

602 **Gene BGLTMP010125 that is hypomethylated by Flv1 shows decreased transcription**

603 One of the identified DMR was particularly intriguing. This DMR that was hypomethylated in Flv1-  
604 treated snails and in their offspring and was close to BGLTMP010125. However, no epiGBS sites were  
605 located within the BGLTMP010125 so that we could not evaluate gene body methylation (GBM) by  
606 this method. We therefore decided to resort to targeted bisulfite sequencing (TBS). We chose a  
607 region in the first intron of the transcript, roughly 2kb upstream of the DMR and spanning 9 CpG to  
608 further explore the relationship between GBM and gene expression. Our TBS results showed that  
609 control snails had five methylated CpG sites in the targeted region of the transcript BGLTMP010125-  
610 RA and that the Flv1-treated snails showed a decrease of the 5mC level in three of the five CpG sites  
611 (Table 6), in the CpG 4 of the control snail 6, the decreased of CpG methylation percentage was from  
612 83.2 to 0%. GBM was significantly lower in Flv1-treated snails ( $t= 10.58$ ,  $df= 8.18$ ,  $p= 4.673e-06$ ) than  
613 in controls (Figure 9a) and the transcript was significantly lower in Flv1-treated samples compared to  
614 controls ( $t= 6.53$ ,  $df= 10.02$ ,  $p=6.477e-05$ ) (Figure 9b).

615

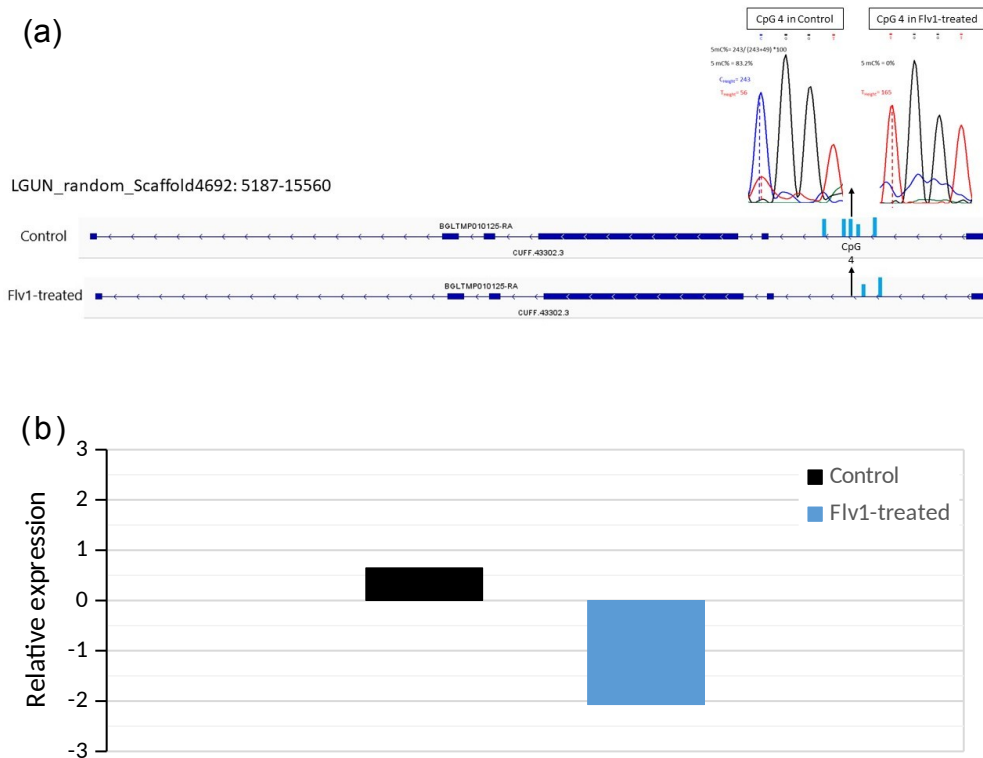
616 **TABLE 6.** 5mC % per CpG sites in the bisulfite converted sequence of the transcript BGLTMP010125.

CpG sites	<i>CpG 1</i>	<i>CpG 2</i>	<i>CpG 3</i>	<i>CpG 4</i>	<i>CpG 5</i>	<i>CpG 6</i>	<i>CpG 7</i>	<i>CpG 8</i>	<i>CpG 9</i>
<b>Position on Contig</b> <b>LGUN_random_Scaffold4692</b>	<i>13866</i>	<i>13976</i>	<i>14024</i>	<i>14042</i>	<i>14059</i>	<i>14061</i>	<i>14317</i>	<i>14331</i>	<i>14343</i>
<b>Control 1</b>	100	0	100	100	0	63.4	0	100	0
<b>Control 2</b>	88.4	0	94.2	83.3	0	62.9	0	95.2	0
<b>Control 3</b>	100	0	97.8	100	0	87.8	0	100	0
<b>Control 4</b>	100	0	100	100	0	40	0	100	0
<b>Control 5</b>	100	0	100	83.1	0	73.4	0	100	0
<b>Control 6</b>	100	0	100	100	0	60	0	100	0
<b>Control 7</b>	89.5	0	95.3	100	0	81.1	0	100	0
<b>Control 8</b>	100	0	100	83.2	0	63.0	0	100	0
<b>Flavanone 1</b>	0	0	0	0	0	79.6	0	76.0	0
<b>Flavanone 2</b>	0		0	0		80.4		100	
<b>Flavanone 3</b>	0	0	0	0	0	54.3	0	93.7	0
<b>Flavanone 4</b>		0		0	0	59.4	0	100	0
<b>Flavanone 5</b>	0	0	0	0	0	60.	0	100	0
<b>Flavanone 6</b>	0	0	0	0	0	71.9	0	100	0
<b>Flavanone 7</b>	0	0	0	0	0	60	0	100	0
<b>Flavanone 8</b>	0	0	0	0	0	68.4	0	100	0
<b>Control mean</b>	97.2	0	98.4	93.7	0	66.4	0	99.4	0
<b>Flavanone mean</b>	0	0	00	0	0	66.7	0	96.2	0

617

618

619



620

621

622 **Figure 9.** (a) Position and level of methylation of the five CpG positions, which has been studied by  
623 TBS within the first intron of the transcript BGLTMP010125-RA. (b) Relative expression of the  
624 transcript BGLTMP010125-RA compared to two housekeeping genes (28S and  $\alpha$ -Tubulin), the  
625 ordinate show the logarithm of the values obtained with the  $2^{-\Delta\Delta CT}$  method.

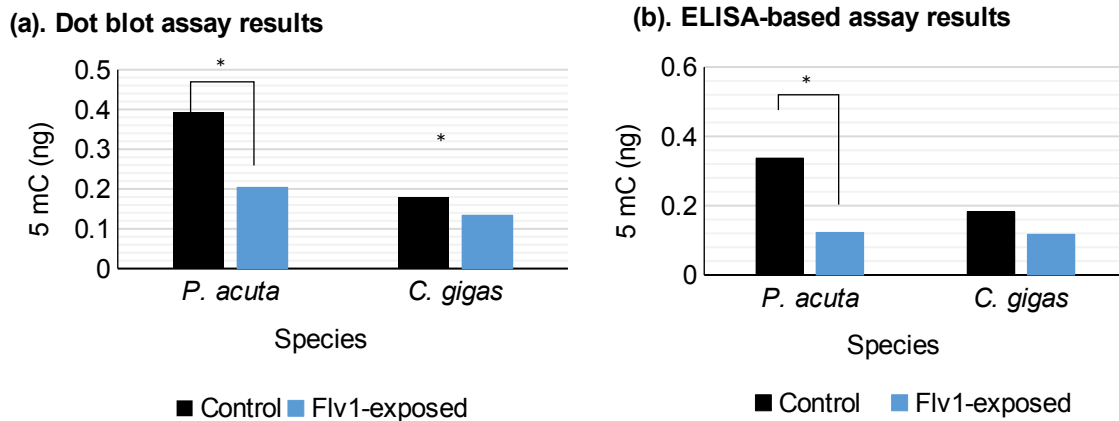
### 626 Flv1 reduces global 5mC in other mollusks

627 Since Flv1 showed efficiency as DNMTi in *B. glabrata* we wondered if it would be active also in other  
628 mollusk species and used *P. acuta* and *C. gigas*. The dot blot results (Figure 10a) displayed that Flv1  
629 exposed *P. acuta* snails have a significantly decreased of the 5mC (ng) concentration compared to  
630 controls ( $t = 5.90, df = 52.23, p = 2.76 \text{ e-}07$ ). For *C. gigas* the decreased in 5mC (ng) by the Flv1  
631 treatment was also significantly different compared to control ( $t = 2.18, df = 47.946, p = 0.0342$ ). The  
632 ELISA results (Figure 10b) showed that the Flv1 compound decreased significantly the 5mC  
633 concentration (ng) in *P. acuta* snails compared to controls ( $t = 4.80, df = 12.33, p = 0.0004$ ), for *C.*

69

70

634 *gigas* we did not find a significantly decrease of the 5mC (ng) ( $t = 1.48$ ,  $df = 12.11$ ,  $p = 0.16$ ) in ELISA-  
 635 based results but we found a tendency to decrease. The reason for this is probably the lower stability  
 636 of Flv1 in sea water (Supplementary file 2, Figure S7).



637

638 **FIGURE 10.** (a) 5mC % measures obtained by the dot blot method for *P. acuta* and *C. gigas*. (b) 5mC  
 639 % measures obtained by the ELISA-based assay. The bars represent the 5mC (ng) mean, the error  
 640 bars represent the standard deviation (SD),  $n = 30$  per group per specie for dot blot and  $n = 10$  for  
 641 ELISA. Significant differences between treatment and control are marked as \* for  $p < 0.05$ .

## 642 Discussion

643 An extension of the concept of inheritance system includes the genotype, the epigenotype, the  
 644 heritable cytoplasmic elements and the microbiome that interacts with the environment to shape  
 645 and transmit the phenotype (Cosseau et al. 2017). The epigenotype and the microbiome can be  
 646 altered by environmental factors and these modifications can be inherited, at least in some systems,  
 647 to later generations, potentially facilitating genetic adaptation. One of the most-studied epigenetic  
 648 mark is DNA methylation. It has been widely studied in vertebrates and plants but remains poorly  
 649 understood in invertebrates, one of the largest phyla of invertebrates are mollusks, that include  
 650 several species that are commercially, ecologically and medically important. It was hypothesized that  
 651 DNA methylation in mollusk can be a mechanism to produce phenotypic variation and potentially

71

72

652 adaptation to new environments (Roberts and Gavery 2012a), but experimental proof is lacking. DNA  
653 methylation in mollusks is likely to be an important element of the inheritance system. One way to  
654 analyze its role is to expose the inheritance system to external perturbations that target specifically  
655 the DNA methylation, *e.g.* by using DNMTi. Such specific inhibitors were synthesized to be used in  
656 human cell lines and they were applied to invertebrates assuming they would have the same effect.  
657 This strategy already led to important advances in other invertebrate species where treatments with  
658 the most used DNMTi, 5-AzaC, were correlated with demethylation and phenotypic changes  
659 (Athanasio et al. 2018, Maharajan et al. 1986, Geyer et al. 2018). Nevertheless, this drug has shown  
660 low response rates, low stability in aqueous solutions and a high toxicity. New DNMTi have been  
661 developed to overcome the weaknesses mentioned above. The aim of this work was to find an  
662 efficient DNMTi for mollusks that (i) provoked minimal side-effects and (ii) allowed the study of the  
663 DNA methylation contribution to phenotypic variability and the heritability of environmental DNA  
664 methylation changes. We tested new generation DNMTi in the snail *B. glabrata* to evaluate their  
665 inhibition potency in a mollusk-like DNA methylation.

666 We used here an antibody-based assay as a screening method of global 5mC % modifications. We  
667 determined a linear correlation between DNA amount and mean spot density in the dot blot assay,  
668 and we demonstrated that it showed comparable results to ELISA-based commercial kit but allowing  
669 the screening of a larger number of samples at a lower price (Supplementary file 2, Figure S5).  
670 Furthermore, we used the epiGBS method for the first time in a mollusk species, providing evidence  
671 that this method can be used to analyze environmental DNA methylation changes genome-wide. This  
672 method allowed the analysis of DNA methylation changes at the nucleotide level of numerous  
673 replicates, that is a prerequisite for ecological studies, at an affordable price and giving results that  
674 represent the same global pattern as WGBS, as shown by the high correlation found between the  
675 methylation ratios of the CpG positions covered by both methods (Spearman correlation,  $R=0.74$ ,

676  $p < 2.2e^{-16}$ ). Besides, epiGBS laboratory protocol and bioinformatics analysis are very flexible and can  
677 be further improved to obtain higher coverage.

#### 678 **Zebularine is not suitable for DNA methylation modification in *B. glabrata***

679 Zebularine has been reported as an efficient DNMT inhibitor in vertebrates, especially in human  
680 cancer cell lines (Tan et al. 2013). In this work we set out to evaluate its effect on the DNA  
681 methylation and phenotypic variation on the snail *B. glabrata*. We decided to use this drug as it is  
682 associated with lower cytotoxicity than the nucleoside analogs (5-AzaC and 5-Aza-deoxycytidine) due  
683 to a different mechanism of action and higher stability in aqueous media (Flotho et al. 2009,  
684 Champion et al. 2015). Nevertheless, the decrease of DNA methylation was not significant following  
685 zebularine treatment. Moreover, we observed an increase in the oviposition of snails treated with  
686 Zebularine (Table 2). This phenomenon was also observed in snails exposed to the parasite *S.*  
687 *mansoni* (Thornhill, Jones, and Kusel 1986), where oviposition is increased during the first days of  
688 parasite exposure. This response may be a fecundity compensatory strategy for expected future  
689 suppression of egg-laying and it is caused by environmental stress and the toxicity of zebularine  
690 possibly triggered this response. Zebularine has demonstrated a transient hypomethylation effect in  
691 plants (Baubec et al. 2009), we cannot exclude that the same could happen in *B. glabrata*, since we  
692 observed some phenotypic effects, especially in the fecundity, presenting the lowest percentage of  
693 hatching rate and a tendency to decrease in the global methylation level. Moreover, zebularine is not  
694 a specific inhibitor of DNMTs, it also inhibits cytidine deaminase, an important enzyme in the  
695 biosynthesis of nucleotides, and most of the compound can be sequestered by this enzyme and  
696 therefore lowering its effective concentration. This is concordant with other studies showing that, in  
697 order to have an effective inhibition of DNMTs, a high concentration of this compound was required  
698 ( $\geq 100 \mu\text{M}$ ) (Cheng et al. 2004).

699 As a nucleoside analogue, the mechanism of action of zebularine requires its incorporation into DNA  
700 after phosphorylation and its conversion to the deoxy-zebularine triphosphate. The new DNMTi  
701 tested in this work are non-nucleoside analogues that do not incorporate into DNA being potentially  
702 more specific to DNMTs (Gros et al. 2012).

703 **Flavanone-type inhibitor has no toxic effects and reduces 5mC level in two subsequent generations**  
704 **associated with variation in morphometric traits**

705 No significant differences were found in the survival and fecundity between Flv1 and its negative  
706 analogue (Flv-neg) against control group. Flv1 triggered a significant decrease on 5mC % in F0  
707 generation and in the F1 generation. Since we found an inhibitory efficiency of the Flv1 in the  
708 mollusks *B. glabrata*, *P. acuta* and *C. gigas*, we decided to test the stability of the flavanone  
709 compounds (3-halo-3-nitroflavanones) in freshwater and in sea saltwater that was used to raise our  
710 mollusks models. We found differences in the chemical stability of Flv1 between freshwater and sea  
711 salt water, the compound was ~3 times more stable in freshwater than it was in sea-salt water  
712 (Supplementary file 2, Figure S7), this can explain the results for *C. gigas* (raised in seawater) were  
713 diminution of global DNA methylation was lower than in the freshwater snails *P. acuta* and *B.*  
714 *glabrata*. Furthermore, we demonstrated an *in vitro* DNMT inhibition activity of the Flv1 compound  
715 in a nuclear extract from *Bge* cells. We concluded that for Flv1, 5mC modulation was most likely due  
716 to direct inhibition of DNMT activity.

717 We corroborated hypomethylation effect in *B. glabrata* by high-throughput bisulfite sequencing with  
718 the epiGBS method, confirming that the average of overall percentage of CpG methylation was  
719 significantly lower in Flv1-exposed snails compared to control and the same trend was found in its  
720 offspring.

721 A total of 26 DMCs (25 hypomethylated and 1 hypermethylated) were found in the Flv1-exposed  
722 snails compared to controls, and its progeny showed 325 DMCs (203 hypomethylated and 120



723 hypermethylated) compared to F1-controls. The higher number of DMCs in the F1 generation, might  
724 be due to an indirect exposure of the germline to the inhibitor. In mollusks, germ cells appear early in  
725 the embryonic development (Luchtel 1972). It has been demonstrated that exposure of the germline  
726 to DNMTi affects epigenetic programming in sperm and oocytes and are likely to affect outcomes and  
727 offspring development principally in vertebrates (Western 2018, Prokopuk, Hogg, and Western  
728 2018). Additionally, the morphometric traits variation was higher in the Flv1-exposed snails and its  
729 offspring. These results are similar to those published in *S. mansoni* (Cosseau et al. 2010), where we  
730 found significant differences in the body length of the parasite larvae between control group and  
731 group treated with the epimutagenic TSA, a histone deacetylase inhibitor. Both results showed that  
732 modification of epigenetic marks by specific drugs can have effects on the phenotype variability of  
733 organisms. Indeed, our results in *B. glabrata* goes in line with the idea that the absence of DNA  
734 methylation could contribute to stochastic transcriptional opportunities and thus be a way to  
735 produce (heritable) phenotypic variability/diversity in mollusks (Roberts and Gavery 2012a).

736 Nevertheless, more work is needed to verify if epimutations at multiple loci are causing the observed  
737 phenotypic variability through post-transcriptional or gene expression changes or if phenotypic  
738 variability is independent of these induced epimutations. Morphometric traits variation is indicative  
739 of growth in mollusks and the heterogeneity of these traits in Flv1-exposed snail's offspring is  
740 coherent with our hypothesis that the germline was indirectly exposed to Flv1.

741 Furthermore, one DMR was observed in Flv1 exposed snails and in its progeny, demonstrating a  
742 multigenerational effect, resulting from a direct exposure of the germline to the inhibitor. Few  
743 examples of multigenerational effect have been reported in mollusks (Fallet et al. 2020), one is our  
744 previous study in *C. gigas* showing that a parental herbicide exposure strongly affected the offspring  
745 DNA methylation pattern (Rondon et al. 2017). Another example was found in *P. acuta*, where  
746 exposure to prednisolone, a steroid hormone evacuated from hospital wastewater, negatively

747 affected the phenotypic traits of the snail, exhibited multigenerational toxicity and affected global  
748 DNA methylation of adult progeny (Bal, Kumar, and Nugegoda 2017).

749 The DMR found in both *B. glabrata* generations mapped to the putative promoter region of  
750 transcript BGLTMP010125 coding for a thump domain-containing protein 3-like. A protein BLAST  
751 (blastp) with the amino acids sequence of this protein showed 66.4% of identity with the THUMP  
752 domain containing protein 3-like of *Aplysia californica* (NCBI reference sequence XP\_012941090) and  
753 52.8% of identity with the THUMP domain protein 3 of the brachiopod *Lingula anatina*  
754 (XP\_013378720.1), these proteins are part of AdoMet\_MTases superfamily, enzymes that use S-  
755 adenosyl-L-methionine (SAM or Adomet) as a substrate for methyltransfer, creating the product S-  
756 adenosyl-L-homocysteine. TBS in the first intron showed that the Flv1 inhibitor treatment decreased  
757 significantly the GBM level in this transcript. qPCR indicted reduced gene expression in Flv1 treated  
758 F0. Our results are in agreement with earlier results in the invertebrates *Nematostella vectensis* and  
759 *Bombyx mori* (Xiang et al. 2010, Zemach et al. 2010), where a positive linear correlation was found  
760 between GBM and mRNA levels.

761 Interestingly, the gene impacted by the inhibitor is coding for a SAM-dependent methyltransferase  
762 whose decreased expression could have leverage effects on 5mC level at multiple loci by influencing  
763 SAM homeostasis.

764 In conclusion, Flv1 is a good candidate to perform multigenerational DNMTi experiments: it did not  
765 impact fecundity neither survival and it induce a DMR found in two consecutive generations. Since  
766 DNMTs are a conserved family of cytosine methyltransferases and since we showed that Flv1  
767 inhibitor is efficient in another two mollusk species *P. acuta* and *C. gigas*, we conclude that this new  
768 DNMTi can be used to pharmacologically modify 5mC level in mollusks species and possibly other  
769 invertebrates, providing a tool to study the inheritance of 5mC environmental modifications.

770 In neo-Darwinian theory, genetic variation is considered a pre-requisite for hereditary phenotypic  
771 variation and as the primary material of adaptation by natural selection. Nevertheless, it has been  
772 demonstrated that the epigenetic inheritance system allows the environmentally induced  
773 phenotypes to be transmitted between generations, which can constitute the basis of adaptative  
774 phenotypic plasticity (Jablonka and Lamb 1999, Jablonka and Lamb 1998). Moreover, epigenetic  
775 changes can be behind rapid adaptive changes observed in scenarios such as climate change,  
776 biological invasions and coevolutionary interactions. However, we need to disentangle the epigenetic  
777 variation from the genetic one and for that we need approaches that allow us to decrease genetic  
778 background and introduce epigenetic changes.

779 Our results hint at epimutations being a source of phenotypic variance that can be induced by  
780 chemicals that disrupt normal mechanisms of methylation control. And this disruption may act on  
781 the germline, with phenotypic expression in the form of heightened phenotypic and epigenetic  
782 variance in the next generation. But we have no proof that variation in methylation patterns are the  
783 only source of the variance in the phenotype found in F0 and F1 generations and we cannot formally  
784 exclude concomitant genetic variation. However, it can now be envisaged to use our new Flv1 DNMTi  
785 to induce epimutations in inbred self-fertilization lines and cross epimutant snails with contrasting  
786 epigenomes (*e.g.* hypomethylated vs hypermethylated snails) allowing to create epigenetic  
787 recombinant inbred lines (epiRILs). In this way one can evaluate if, in the absence of genetic  
788 variation, epimutations and phenotypic variation induced in the exposed generations are transmitted  
789 across multiple generations and produce phenotypes having a selective advantage.

790

791 **Figure and table legends.**

792 **FIGURE 1.** 5mC % of *B. glabrata* snails upon DNMTi treatments at a concentration of 10  $\mu$ M, error  
793 bars represent SD, n=30 per treatment.

794 **FIGURE 2.** Kaplan-Meier survival curves upon treatment with the two types of DNMTi.

795 **FIGURE 3.** PCA of morphometric traits of all treatments of F0 (a) and F1 generation (b).

796 **FIGURE 4.** Histograms of CpG methylation distribution, (a) histogram of F0-control epiGBS libraries  
797 (b) histogram of F1-control epiGBS libraries and (c) histogram of WGBS library.

798 **FIGURE 5.** Screenshot of IGV of the region LGUN\_random\_Scaffold28: 1-800 Kb, that showed the  
799 regions covered by epiGBS libraries (in yellow) versus the regions covered by WGBS library (blue).

800 **FIGURE 6.** CpG methylation ratio profile across the bodies of genes and quantiles distribution of  
801 epiGBS and WGBS libraries

802 **FIGURE 7.** PCA of CpG methylation of the Flv1-treated and control groups in F0 generation (a) and in  
803 its offspring (b).

804 **Figure 8.** IGV screenshot of the LGUN\_random\_scaffold4962:16175-16266 of *B. glabrata* genome  
805 assembly (GCA\_000457365.1).

806 **Figure 9.** (a) Position and level of methylation of the five CpG positions, which has been studied by  
807 TBS within the first intron of the transcript BGLTMP010125-RA. (b) Relative expression of the  
808 transcript BGLTMP010125-RA compared to two housekeeping genes (28S and  $\alpha$ -Tubulin), the  
809 ordinate show the logarithm of the values obtained with the  $2^{-\Delta\Delta CT}$  method.

810 **FIGURE 10.** (a) 5mC % measures obtained by the dot blot method for *P. acuta* and *C. gigas*. (b) 5mC  
811 % measures obtained by the ELISA-based assay.

812 **TABLE 1.** *Biomphalaria glabarata* gene-specific primers used to amplified gene fragments used in the  
813 RT-qPCR.

814 **TABLE 2.** Contingency table of fecundity of the snails exposed to different DNMTi.

815 **TABLE 3.** Mapping efficiencies, CpG coverage and average genome-wide methylation levels resulting  
816 from epiGBS and WGBS libraries.

817 **TABLE 4.** Percentage of CpG methylation sites which display an unmethylated or complete  
818 methylated pattern.

819 **Table 5.** DMCs in Flv1-treated and control group for each generation.

820 **TABLE6.** 5mC % per CpG sites in the bisulfite converted sequence of the transcript BGLTMP010125.  
821

822 **Abbreviations**

823 6-FAM: 6-Carboxyfluorescein

824 THUMP: THioUridine synthases, RNA Methyltransferases and Pseudo-uridine synthases

825 AdoMeth or SAM: S-adenosyl-L-methionine

826 5mC: 5-methylcytosine

827 DNMTs: DNA methyltransferases

828 DNMTi: DNA methyltransferase inhibitors

829 5-AzaC: 5-azacytidine

830 BgBRE: *Biomphalaria glabrata* strain Brazil BRE

831 Bge: *Biomphalaria glabrata* embryonic

832 **Ethics approval and consent to participate**

833 The Direction Départementale de la Cohésion Sociale et de la Protection des Populations (DDSCPP)

834 provided the permit N°C66-136-01 to IHPE for experiments on animals.

835 **Consent for publication**

836 All authors read and endorsed the manuscript.

837 **Availability of data and materials**

838 All Flv substrates are available on request. Raw data is available at NCBI SRA XXXXXX (provided on

839 accepted version)

840 **Competing interests**

841 The authors declare no conflict of interest.

842 **Funding**

843 This work was supported by Wellcome Trust strategic award [107475/Z/15/Z] and by a PhD grant to

844 NL from the Region Occitanie (EPIPAPA project) and the University of Perpignan Via Domitia graduate

845 school ED305. With the support of LabEx CeMEB, an ANR “Investissements d’avenir” program (ANR-  
846 10-LABX-04-01) through the Environmental Epigenomics Platform and the “projets de recherche  
847 exploratoires du CeMEB 2018” project “Epigenetics of inbreeding depression (EPID)”. This study is set  
848 within the framework of the "Laboratoires d'Excellences (LABEX)" TULIP (ANR-10-LABX-41)

#### 849 **Authors' contributions**

850 CG and CC designed the study, analyze data and writing the manuscript. NL performed the  
851 experimental work, processed and analyses data and wrote the manuscript. ML and PBA synthesized  
852 the chemical compounds used in this study, elaborate the chemical stability and *in vitro* inhibition  
853 assays and participate in the writing of the manuscript. SI helped in the elaboration of epiGBS  
854 libraries. KV and FG help in the analysis of epiGBS sequencing reads and participate in the writing of  
855 the manuscript. PD participated in the experimental design and in the writing of the manuscript. CrC  
856 help with the bioinformatics analysis.

#### 857 **Acknowledgements**

858 We are very grateful to R. Galinier and M. Fallet for their support during the optimization of the  
859 protocol to measure DNA methylation and to N. Arancibia for breeding of mollusks. We thank L.  
860 Halby for its contribution to the discussion of this manuscript and for synthesized compounds used in  
861 the screening of effective DNMTi. We thank J.F. Allienne at the Bio-environment platform (University  
862 Perpignan Via Domitia) for support in NGS library preparation and sequencing. We thank B. Petton  
863 for the breeding of juvenile oysters used in this study and we thank G. Rico for her help in the  
864 analysis of dot blot and ELISA of *P. acuta* and *C. gigas*.

865

866

#### 867 **References**

89

90

868 Adema, C. M., L. W. Hillier, C. S. Jones, E. S. Loker, M. Knight, P. Minx, G. Oliveira, N. Raghavan, A.  
869 Shedlock, L. R. do Amaral, H. D. Arican-Goktas, J. G. Assis, E. H. Baba, O. L. Baron, C. J. Bayne,  
870 U. Bickham-Wright, K. K. Biggar, M. Blouin, B. C. Bonning, C. Botka, J. M. Bridger, K. M.  
871 Buckley, S. K. Buddenborg, R. Lima Caldeira, J. Carleton, O. S. Carvalho, M. G. Castillo, I. W.  
872 Chalmers, M. Christensens, S. Clifton, C. Cosseau, C. Coustau, R. M. Cripps, Y. Cuesta-Astroz,  
873 S. F. Cummins, L. di Stephano, N. Dinguirard, D. Duval, S. Emrich, C. Feschotte, R. Feyereisen,  
874 P. FitzGerald, C. Fronick, L. Fulton, R. Galinier, S. G. Gava, M. Geusz, K. K. Geyer, G. I. Giraldo-  
875 Calderón, M. de Souza Gomes, M. A. Gordy, B. Gourbal, C. Grunau, P. C. Hanington, K. F.  
876 Hoffmann, D. Hughes, J. Humphries, D. J. Jackson, L. K. Jannotti-Passos, W. de Jesus Jeremias,  
877 S. Jobling, B. Kamel, A. Kapusta, S. Kaur, J. M. Koene, A. B. Kohn, D. Lawson, S. P. Lawton, D.  
878 Liang, Y. Limpanont, S. Liu, A. E. Lockyer, T. L. Lovato, F. Ludolf, V. Magrini, D. P. McManus,  
879 M. Medina, M. Misra, G. Mitta, G. M. Mkoji, M. J. Montague, C. Montelongo, L. L. Moroz, M.  
880 C. Munoz-Torres, U. Niazi, L. R. Noble, F. S. Oliveira, F. S. Pais, A. T. Papenfuss, R. Peace, J. J.  
881 Pena, E. A. Pila, T. Quelais, B. J. Raney, J. P. Rast, D. Rollinson, I. C. Rosse, B. Rotgans, E. J.  
882 Routledge, K. M. Ryan, L. L. S. Scholte, K. B. Storey, M. Swain, J. A. Tennessen, C. Tomlinson,  
883 D. L. Trujillo, E. V. Volpi, A. J. Walker, T. Wang, I. Wannaporn, W. C. Warren, X. J. Wu, T. P.  
884 Yoshino, M. Yusuf, S. M. Zhang, M. Zhao, and R. K. Wilson. 2017. "Whole genome analysis of  
885 a schistosomiasis-transmitting freshwater snail." *Nat Commun* 8:15451. doi:  
886 10.1038/ncomms15451.

887 Akalin, A., M. Kormaksson, S. Li, F. E. Garrett-Bakelman, M. E. Figueroa, A. Melnick, and C. E. Mason.  
888 2012. "methylKit: a comprehensive R package for the analysis of genome-wide DNA  
889 methylation profiles." *Genome Biol* 13 (10):R87. doi: 10.1186/gb-2012-13-10-r87.

890 Aliaga, B., I. Bulla, G. Mouahid, D. Duval, and C. Grunau. 2019. "Universality of the DNA methylation  
891 codes in Eucaryotes." *Sci Rep* 9 (1):173. doi: 10.1038/s41598-018-37407-8.

892 Allan, E. R. O., S. Bollmann, E. Peremyslova, and M. Blouin. 2020. "Neither heat pulse, nor  
893 multigenerational exposure to a modest increase in water temperature, alters the  
894 susceptibility of Guadeloupean." *PeerJ* 8:e9059. doi: 10.7717/peerj.9059.

895 Athanasio, C. G., U. Sommer, M. R. Viant, J. K. Chipman, and L. Mirbahai. 2018. "Use of 5-azacytidine  
896 in a proof-of-concept study to evaluate the impact of pre-natal and post-natal exposures, as  
897 well as within generation persistent DNA methylation changes in *Daphnia*." *Ecotoxicology* 27  
898 (5):556-568. doi: 10.1007/s10646-018-1927-3.

899 Baccarelli, A., and V. Bollati. 2009. "Epigenetics and environmental chemicals." *Curr Opin Pediatr* 21  
900 (2):243-51.

901 Bal, N., A. Kumar, and D. Nugegoda. 2017. "Assessing multigenerational effects of prednisolone to  
902 the freshwater snail, *Physa acuta* (Gastropoda: Physidae)." *J Hazard Mater* 339:281-291. doi:  
903 10.1016/j.jhazmat.2017.06.024.

904 Baubec, T., A. Pecinka, W. Rozhon, and O. Mittelsten Scheid. 2009. "Effective, homogeneous and  
905 transient interference with cytosine methylation in plant genomic DNA by zebularine." *Plant*  
906 *J* 57 (3):542-54. doi: 10.1111/j.1365-313X.2008.03699.x.

907 Bossdorf, O., C. L. Richards, and M. Pigliucci. 2008. "Epigenetics for ecologists." *Ecol Lett* 11 (2):106-  
908 15. doi: 10.1111/j.1461-0248.2007.01130.x.

909 Boyd, V. L., and G. Zon. 2004. "Bisulfite conversion of genomic DNA for methylation analysis: protocol  
910 simplification with higher recovery applicable to limited samples and increased throughput."  
911 *Anal Biochem* 326 (2):278-80. doi: 10.1016/j.ab.2003.11.020.

912 Capuano, F., M. Mülleder, R. Kok, H. J. Blom, and M. Ralser. 2014. "Cytosine DNA methylation is  
913 found in *Drosophila melanogaster* but absent in *Saccharomyces cerevisiae*,  
914 *Schizosaccharomyces pombe*, and other yeast species." *Anal Chem* 86 (8):3697-702. doi:  
915 10.1021/ac500447w.

916 Carvalho, S., R. L. Caldeira, A. J. Simpson, and T. H. Vidigal. 2001. "Genetic variability and molecular  
917 identification of Brazilian Biomphalaria species (Mollusca: Planorbidae)." *Parasitology* 123  
918 Suppl:S197-209. doi: 10.1017/s0031182001008058.

919 Ceccaldi, A., A. Rajavelu, C. Champion, C. Rampon, R. Jurkowska, G. Jankevicius, C. Senamaud-  
920 Beaufort, L. Ponger, N. Gagey, H. D. Ali, J. Tost, S. Vriza, S. Ros, D. Dauzonne, A. Jeltsch, D.  
921 Guianvarc'h, and P. B. Arimondo. 2011. "C5-DNA methyltransferase inhibitors: from  
922 screening to effects on zebrafish embryo development." *Chembiochem* 12 (9):1337-45. doi:  
923 10.1002/cbic.201100130.

924 Champion, C., Guianvarc'h, D., Sénamaud-Beaufort, C., Jurkowska, R. Z., Jeltsch, A., Ponger, L., . . .  
925 Guiesse-Peugeot, A. L. (2010). Mechanistic insights on the inhibition of c5 DNA  
926 methyltransferases by zebularine. *PLoS One*, 5(8), e12388.  
927 doi:10.1371/journal.pone.0012388

928 Chen, T. 2011. "Mechanistic and functional links between histone methylation and DNA  
929 methylation." *Prog Mol Biol Transl Sci* 101:335-48. doi: 10.1016/B978-0-12-387685-0.00010-  
930 X.

931 Cheng, J. C., D. J. Weisenberger, F. A. Gonzales, G. Liang, G. L. Xu, Y. G. Hu, V. E. Marquez, and P. A.  
932 Jones. 2004. "Continuous zebularine treatment effectively sustains demethylation in human  
933 bladder cancer cells." *Mol Cell Biol* 24 (3):1270-8.

934 Cosseau, C., O. Wolkenhauer, G. Padalino, K. K. Geyer, K. F. Hoffmann, and C. Grunau. 2017.  
935 "(Epi)genetic Inheritance in *Schistosoma mansoni*: A Systems Approach." *Trends Parasitol* 33  
936 (4):285-294. doi: 10.1016/j.pt.2016.12.002.

937 Cosseau, C., A. Azzi, A. Rognon, J. Boissier, S. Gourbiere, E. Roger, G. Mitta, and C. Grunau. 2010.  
938 "Epigenetic and phenotypic variability in populations of *Schistosoma mansoni*—a possible  
939 kick-off for adaptive host/parasite evolution." *Oikos* 119 (4):669-678.

940 de Lorgeteril, J., A. Lucasson, B. Petton, E. Toulza, C. Montagnani, C. Clerissi, J. Vidal-Dupiol, C.  
941 Chaparro, R. Galinier, J.-Michel Escoubas, P. Haffner, L. Dégremont, G. M. Charrière, M.  
942 Lafont, A. Delort, A. Vergnes, M. Chiarello, N. Faury, T. Rubio, M. A. Leroy, A. Pérignon,  
943 D.Régler, B. Morga, M. Alunno-Bruscia, P. Boudry, F. Le Roux, D. Destoumieux-Garzón, Y.  
944 Gueguen, and G. Mitta. 2018. "Immune-suppression by OsHV-1 viral infection causes fatal  
945 bacteraemia in Pacific oysters." *Nature Communications* 9 (1):4215. doi: 10.1038/s41467-  
946 018-06659-3.

947 Diala, E. S., and R. M. Hoffman. 1982. "Hypomethylation of HeLa cell DNA and the absence of 5-  
948 methylcytosine in SV40 and adenovirus (type 2) DNA: analysis by HPLC." *Biochem Biophys*  
949 *Res Commun* 107 (1):19-26.

950 Dreyfuss, G., P. Vignoles, M. Abrous, and D. Rondelaud. 2002. "Unusual snail species involved in the  
951 transmission of *Fasciola hepatica* in watercress beds in central France." *Parasite* 9 (2):113-  
952 20. doi: 10.1051/parasite/2002092113.

953 Dupont, C., D. R. Armant, and C. A. Brenner. 2009. "Epigenetics: definition, mechanisms and clinical  
954 perspective." *Semin Reprod Med* 27 (5):351-7. doi: 10.1055/s-0029-1237423.

955 Erdmann, A., Halby, L., Fahy, J., & Arimondo, P. B. (2015). Targeting DNA Methylation with Small  
956 Molecules: What's Next? *Journal of Medicinal Chemistry*, 58(6), 2569-2583.  
957 doi:10.1021/jm500843d

958 Fallet, M., E. Luquet, P. David, and C. Cosseau. 2020. "Epigenetic inheritance and intergenerational  
959 effects in mollusks." *Gene* 729:144166. doi: 10.1016/j.gene.2019.144166.

960 Feng, S., S. J. Cokus, X. Zhang, P. Y. Chen, M. Bostick, M. G. Goll, J. Hetzel, J. Jain, S. H. Strauss, M. E.  
961 Halpern, C. Ukomadu, K. C. Sadler, S. Pradhan, M. Pellegrini, and S. E. Jacobsen. 2010.  
962 "Conservation and divergence of methylation patterning in plants and animals." *Proc Natl*  
963 *Acad Sci U S A* 107 (19):8689-94. doi: 10.1073/pnas.1002720107.



964 Flotho, C., R. Claus, C. Batz, M. Schneider, I. Sandrock, S. Ihde, C. Plass, C. M. Niemeyer, and M.  
965 Lübbert. 2009. "The DNA methyltransferase inhibitors azacitidine, decitabine and zebularine  
966 exert differential effects on cancer gene expression in acute myeloid leukemia cells."  
967 *Leukemia* 23 (6):1019-28. doi: 10.1038/leu.2008.397.

968 Fneich, S., N. Dheilly, C. Adema, A. Rognon, M. Reichelt, J. Bulla, C. Grunau, and C. Cosseau. 2013. "5-  
969 methyl-cytosine and 5-hydroxy-methyl-cytosine in the genome of *Biomphalaria glabrata*, a  
970 snail intermediate host of *Schistosoma mansoni*." *Parasites & vectors* 6 (1):167.

971 Frommer, M., L. E. McDonald, D. S. Millar, C. M. Collis, F. Watt, G. W. Grigg, P. L. Molloy, and C. L.  
972 Paul. 1992. "A genomic sequencing protocol that yields a positive display of 5-methylcytosine  
973 residues in individual DNA strands." *Proc Natl Acad Sci U S A* 89 (5):1827-31.

974 Ganesan, A., Arimondo, P. B., Rots, M. G., Jeronimo, C., & Berdasco, M. (2019). The timeline of  
975 epigenetic drug discovery: from reality to dreams. *Clinical Epigenetics*, 11(1), 174.

976 Gawehns, Fleur, M. Postuma, T. P van Gurp, N. CAM Wagemaker, S. Fatma, M. Van Antro, C.  
977 Mateman, S. Milanovic-Ivanovic, K. van Oers, and I. Große. 2020. "epiGBS2: an improved  
978 protocol and automated snakemake workflow for highly multiplexed reduced representation  
979 bisulfite sequencing." *bioRxiv*.

980 Geyer, K. K., S. E. Munshi, M. Vickers, M. Squance, T. J. Wilkinson, D. Berrar, C. Chaparro, M. T. Swain,  
981 and K. F. Hoffmann. 2018. "The anti-fecundity effect of 5-azacytidine (5-AzaC) on  
982 *Schistosoma mansoni* is linked to dis-regulated transcription, translation and stem cell  
983 activities." *Int J Parasitol Drugs Drug Resist* 8 (2):213-222. doi: 10.1016/j.ijpddr.2018.03.006.

984 Geyer, K. K., U. H. Niazi, D. Duval, C. Cosseau, C. Tomlinson, I. W. Chalmers, M. T. Swain, D. J. Cutress,  
985 U. Bickham-Wright, S. E. Munshi, C. Grunau, T. P. Yoshino, and K. F. Hoffmann. 2017. "The  
986 *Biomphalaria glabrata* DNA methylation machinery displays spatial tissue expression, is  
987 differentially active in distinct snail populations and is modulated by interactions with  
988 *Schistosoma mansoni*." *PLoS Negl Trop Dis* 11 (5):e0005246. doi:  
989 10.1371/journal.pntd.0005246.

990 Geyer, K. K., C. M. Rodríguez López, I. W. Chalmers, S. E. Munshi, M. Truscott, J. Heald, M. J.  
991 Wilkinson, and K. F. Hoffmann. 2011. "Cytosine methylation regulates oviposition in the  
992 pathogenic blood fluke *Schistosoma mansoni*." *Nat Commun* 2:424. doi:  
993 10.1038/ncomms1433.

994 Glastad, K. M., B. G. Hunt, S. V. Yi, and M. A. Goodisman. 2011. "DNA methylation in insects: on the  
995 brink of the epigenomic era." *Insect Mol Biol* 20 (5):553-65. doi: 10.1111/j.1365-  
996 2583.2011.01092.x.

997 Gnyszka, A., Z. Jastrzebski, and S. Flis. 2013. "DNA methyltransferase inhibitors and their emerging  
998 role in epigenetic therapy of cancer." *Anticancer Res* 33 (8):2989-96.

999 Gowher, H., O. Leismann, and A. Jeltsch. 2000. "DNA of *Drosophila melanogaster* contains 5-  
1000 methylcytosine." *EMBO J* 19 (24):6918-23. doi: 10.1093/emboj/19.24.6918.

1001 Gros, C., J. Fahy, L. Halby, I. Dufau, A. Erdmann, J. M. Gregoire, F. Ausseil, S. Vispé, and P. B.  
1002 Arimondo. 2012. "DNA methylation inhibitors in cancer: recent and future approaches."  
1003 *Biochimie* 94 (11):2280-96. doi: 10.1016/j.biochi.2012.07.025.

1004 Grunau, C., S. J. Clark, and A. Rosenthal. 2001. "Bisulfite genomic sequencing: systematic  
1005 investigation of critical experimental parameters." *Nucleic Acids Res* 29 (13):E65-5. doi:  
1006 10.1093/nar/29.13.e65.

1007 Halby, L., Y. Menon, E. Rilova, D. Pechalrieu, V. Masson, C. Faux, M. A. Bouhleh, M. H. David-  
1008 Cordonnier, N. Novosad, Y. Aussagues, A. Samson, L. Lacroix, F. Ausseil, L. Fleury, D.  
1009 Guianvarc'h, C. Ferroud, and P. B. Arimondo. 2017. "Rational Design of Bisubstrate-Type  
1010 Analogues as Inhibitors of DNA Methyltransferases in Cancer Cells." *J Med Chem* 60  
1011 (11):4665-4679. doi: 10.1021/acs.jmedchem.7b00176.

1012 Hendrich, B., and S. Tweedie. 2003. "The methyl-CpG binding domain and the evolving role of DNA  
1013 methylation in animals." *Trends Genet* 19 (5):269-77. doi: 10.1016/S0168-9525(03)00080-5.

1014 Jablonka, E., and M. J. Lamb. 1998. "Epigenetic inheritance in evolution." *Journal of Evolutionary*  
1015 *Biology* 11 (2):159-183. doi: 10.1046/j.1420-9101.1998.11020159.x.

1016 Jablonka, E., and M. J. Lamb. 1999. *Epigenetic inheritance and evolution: the Lamarckian dimension:*  
1017 Oxford University Press on Demand.

1018 Jiang, M., Y. Zhang, J. Fei, X. Chang, W. Fan, X. Qian, T. Zhang, and D. Lu. 2010. "Rapid quantification  
1019 of DNA methylation by measuring relative peak heights in direct bisulfite-PCR sequencing  
1020 traces." *Lab Invest* 90 (2):282-90. doi: 10.1038/labinvest.2009.132.

1021 Johannes, F., E. Porcher, F. K. Teixeira, V. Saliba-Colombani, M. Simon, N. Agier, A. Bulski, J.  
1022 Albuissou, F. Heredia, P. Audigier, D. Bouchez, C. Dillmann, P. Guerche, F. Hospital, and V.  
1023 Colot. 2009. "Assessing the impact of transgenerational epigenetic variation on complex  
1024 traits." *PLoS Genet* 5 (6):e1000530. doi: 10.1371/journal.pgen.1000530.

1025 Jozefczuk, J., and James Adjaye. 2011. "Quantitative real-time PCR-based analysis of gene expression."  
1026 In *Methods in enzymology*, 99-109. Elsevier.

1027 Kanev, I. 1994. "Life-cycle, delimitation and redescription of *Echinostoma revolutum* (Froelich, 1802)  
1028 (Trematoda: Echinostomatidae)." *Systematic Parasitology* 28 (2):125-144.

1029 Keller, T. E., P. Han, and S. V. Yi. 2016. "Evolutionary Transition of Promoter and Gene Body DNA  
1030 Methylation across Invertebrate-Vertebrate Boundary." *Mol Biol Evol* 33 (4):1019-28. doi:  
1031 10.1093/molbev/msv345.

1032 Knight, M., W. Ittiprasert, H. D. Arican-Goktas, and J. M. Bridger. 2016. "Epigenetic modulation, stress  
1033 and plasticity in susceptibility of the snail host, *Biomphalaria glabrata*, to *Schistosoma*  
1034 *mansonii* infection." *Int J Parasitol* 46 (7):389-94. doi: 10.1016/j.ijpara.2016.03.003.

1035 Krueger, F. 2012. "Trim Galore: a wrapper tool around Cutadapt and FastQC to consistently apply  
1036 quality and adapter trimming to FastQ files, with some extra functionality for MspI-digested  
1037 RRBS-type (Reduced Representation Bisulfite-Seq) libraries." URL [http://www.](http://www.bioinformatics.babraham.ac.uk/projects/trim_galore/)  
1038 [bioinformatics.babraham.ac.uk/projects/trim\\_galore/](http://www.bioinformatics.babraham.ac.uk/projects/trim_galore/). (Date of access: 28/04/2016).

1039 Li, E., and Y. Zhang. 2014. "DNA methylation in mammals." *Cold Spring Harb Perspect Biol* 6  
1040 (5):a019133. doi: 10.1101/cshperspect.a019133.

1041 Li, L. C., and R. Dahiya. 2002. "MethPrimer: designing primers for methylation PCRs." *Bioinformatics*  
1042 18 (11):1427-31. doi: 10.1093/bioinformatics/18.11.1427.

1043 Lopez, M., L. Halby, and P. B. Arimondo. 2016. "DNA Methyltransferase Inhibitors: Development and  
1044 Applications." *Adv Exp Med Biol* 945:431-473. doi: 10.1007/978-3-319-43624-1\_16.

1045 Luchtel, D. 1972. "Gonadal development and sex determination in pulmonate molluscs. I. *Arion*  
1046 *circumscriptus*." *Z Zellforsch Mikrosk Anat* 130 (3):279-301. doi: 10.1007/bf00306943.

1047 Luviano, N., S. Diaz-Palma, C. Cosseau, and C. Grunau. 2018. "A simple Dot Blot Assay for population  
1048 scale screening of DNA methylation." *bioRxiv*:454439. doi: 10.1101/454439.

1049 Maharajan, P., V. Maharajan, M. Branno, and E. Scarano. 1986. "Effects of 5 azacytidine on DNA  
1050 methylation and early development of sea urchins and ascidia." *Differentiation* 32 (3):200-7.

1051 McManus, D. P. (2019). Defeating Schistosomiasis. *New England Journal of Medicine*, 381(26), 2567-  
1052 2568. doi:10.1056/NEJMe1913771

1053 Meng, H., Y. Cao, J. Qin, X. Song, Q. Zhang, Y. Shi, and L. Cao. 2015. "DNA methylation, its mediators  
1054 and genome integrity." *Int J Biol Sci* 11 (5):604-17. doi: 10.7150/ijbs.11218.

1055 Meröndun, J., D. L. Murray, and A. B. A. Shafer. 2019. "Genome-scale sampling suggests cryptic  
1056 epigenetic structuring and insular divergence in *Canada lynx*." *Mol Ecol* 28 (13):3186-3196.  
1057 doi: 10.1111/mec.15131.

1058 Moore, L. D., T. Le, and G. Fan. 2013. "DNA methylation and its basic function."  
1059 *Neuropsychopharmacology* 38 (1):23-38. doi: 10.1038/npp.2012.112.

- 1060 Müller, R., S. Charaf, C. Scherer, A. Oppold, J. Oehlmann, and M. Wagner. 2016. "Phenotypic and  
1061 epigenetic effects of vinclozolin in the gastropod *Physella acuta*." *Journal of Molluscan*  
1062 *Studies* 82 (2):320-327. doi: 10.1093/mollus/eyv069.
- 1063 Nicoglou, A., and F. Merlin. 2017. "Epigenetics: A way to bridge the gap between biological fields."  
1064 *Stud Hist Philos Biol Biomed Sci* 66:73-82. doi: 10.1016/j.shpsc.2017.10.002.
- 1065 Pechalrieu, D., Etievant, C., & Arimondo, P. B. (2017). DNA methyltransferase inhibitors in cancer:  
1066 From pharmacology to translational studies. *Biochem Pharmacol*, 129, 1-13.  
1067 doi:10.1016/j.bcp.2016.12.004
- 1068 Pechalrieu, D., D. Dauzonne, P. B. Arimondo, and M. Lopez. 2020. "Synthesis of novel 3-halo-3-  
1069 nitroflavanones and their activities as DNA methyltransferase inhibitors in cancer cells." *Eur J*  
1070 *Med Chem* 186:111829. doi: 10.1016/j.ejmech.2019.111829.
- 1071 Prokopuk, L., K. Hogg, and P. S. Western. 2018. "Pharmacological inhibition of EZH2 disrupts the  
1072 female germline epigenome." *Clin Epigenetics* 10:33. doi: 10.1186/s13148-018-0465-4.
- 1073 Reamon-Buettner, S. M., V. Mutschler, and J. Borlak. 2008. "The next innovation cycle in  
1074 toxicogenomics: environmental epigenetics." *Mutat Res* 659 (1-2):158-65. doi:  
1075 10.1016/j.mrrev.2008.01.003.
- 1076 Rivière, G. 2014. "Epigenetic features in the oyster *Crassostrea gigas* suggestive of functionally  
1077 relevant promoter DNA methylation in invertebrates." *Frontiers in physiology* 5:129.
- 1078 Roberts, S. B., and M. R. Gavery. 2012a. "Is There a Relationship between DNA Methylation and  
1079 Phenotypic Plasticity in Invertebrates?" *Front Physiol* 2:116. doi: 10.3389/fphys.2011.00116.
- 1080 Roberts, S. B, and Mackenzie R Gavery. 2012b. "Is there a relationship between DNA methylation and  
1081 phenotypic plasticity in invertebrates?" *Frontiers in physiology* 2:116.
- 1082 Rondon, R., C. Grunau, M. Fallet, N. Charlemagne, R. Sussarellu, C. Chaparro, C. Montagnani, G.  
1083 Mitta, E. Bachère, F. Akcha, and C. Cosseau. 2017. "Effects of a parental exposure to diuron  
1084 on Pacific oyster spat methylome." *Environ Epigenet* 3 (1):dvx004. doi: 10.1093/eep/dvx004.
- 1085 Sarda, S., J. Zeng, B. G Hunt, and V Yi Soojin. 2012. "The evolution of invertebrate gene body  
1086 methylation." *Molecular biology and evolution* 29 (8):1907-1916.
- 1087 Schübeler, D. 2015. "Function and information content of DNA methylation." *Nature* 517 (7534):321-  
1088 6. doi: 10.1038/nature14192.
- 1089 Seeland, A., J. Albrand, J. Oehlmann, and R. Müller. 2013. "Life stage-specific effects of the fungicide  
1090 pyrimethanil and temperature on the snail *Physella acuta* (Draparnaud, 1805) disclose the  
1091 pitfalls for the aquatic risk assessment under global climate change." *Environmental*  
1092 *Pollution* 174:1-9.
- 1093 Sullivan, J. 2018. "Reversal of schistosome resistance in *Biomphalaria glabrata* by heat shock may be  
1094 dependent on snail genotype." *J Parasitol*. doi: 10.1645/17-110.
- 1095 Suzuki, M. M., and A. Bird. 2008. "DNA methylation landscapes: provocative insights from  
1096 epigenomics." *Nat Rev Genet* 9 (6):465-76. doi: 10.1038/nrg2341.
- 1097 Tan, W., W. Zhou, H. G. Yu, H. S. Luo, and L. Shen. 2013. "The DNA methyltransferase inhibitor  
1098 zebularine induces mitochondria-mediated apoptosis in gastric cancer cells in vitro and in  
1099 vivo." *Biochem Biophys Res Commun* 430 (1):250-5. doi: 10.1016/j.bbrc.2012.10.143.
- 1100 Theron, A., A. Rognon, B. Gourbal, and G. Mitta. 2014. "Multi-parasite host susceptibility and multi-  
1101 host parasite infectivity: a new approach of the *Biomphalaria glabrata*/*Schistosoma mansoni*  
1102 compatibility polymorphism." *Infect Genet Evol* 26:80-8. doi: 10.1016/j.meegid.2014.04.025.
- 1103 Thornhill, J. A., J. T. Jones, and J. R. Kusel. 1986. "Increased oviposition and growth in immature  
1104 *Biomphalaria glabrata* after exposure to *Schistosoma mansoni*." *Parasitology* 93 ( Pt 3):443-  
1105 50.
- 1106 Ueno, M., K. Katayama, H. Nakayama, and K. Doi. 2002. "Mechanisms of 5-azacytidine (5AzC)-  
1107 induced toxicity in the rat foetal brain." *Int J Exp Pathol* 83 (3):139-50. doi: 10.1046/j.1365-  
1108 2613.2002.00225.x.

- 1109 van Gorp, T. P., N. C. Wagemaker, B. Wouters, P. Vergeer, J. N. Ouborg, and K. J. Verhoeven. 2016.  
1110 "epiGBS: reference-free reduced representation bisulfite sequencing." *Nat Methods* 13  
1111 (4):322-4. doi: 10.1038/nmeth.3763.
- 1112 Vinarski, M. V. 2017. "The history of an invasion: phases of the explosive spread of the physid snail  
1113 *Physella acuta* through Europe, Transcaucasia and Central Asia." *Biological invasions* 19  
1114 (4):1299-1314.
- 1115 Western, P. S. 2018. "Epigenomic drugs and the germline: Collateral damage in the home of  
1116 heritability?" *Mol Cell Endocrinol* 468:121-133. doi: 10.1016/j.mce.2018.02.008.
- 1117 Xi, Y., and W. Li. 2009. "BSMAP: whole genome bisulfite sequence MAPping program." *BMC*  
1118 *Bioinformatics* 10:232. doi: 10.1186/1471-2105-10-232.
- 1119 Xiang, H., J. Zhu, Q. Chen, F. Dai, X. Li, M. Li, H. Zhang, G. Zhang, D. Li, Y. Dong, L. Zhao, Y. Lin, D.  
1120 Cheng, J. Yu, J. Sun, X. Zhou, K. Ma, Y. He, Y. Zhao, S. Guo, M. Ye, G. Guo, Y. Li, R. Li, X. Zhang,  
1121 L. Ma, K. Kristiansen, Q. Guo, J. Jiang, S. Beck, Q. Xia, W. Wang, and J. Wang. 2010. "Single  
1122 base-resolution methylome of the silkworm reveals a sparse epigenomic map." *Nat*  
1123 *Biotechnol* 28 (5):516-20. doi: 10.1038/nbt.1626.
- 1124 Zemach, A., I.E McDaniel, P. Silva, and D. Zilberman. 2010. "Genome-wide evolutionary analysis of  
1125 eukaryotic DNA methylation." *Science* 328 (5980):916-919.
- 1126 Zilberman, D. 2008. "The evolving functions of DNA methylation." *Curr Opin Plant Biol* 11 (5):554-9.  
1127 doi: 10.1016/j.pbi.2008.07.004.

1128